Protoplanetary Disks and their Evolution

Jonathan P. Williams and Lucas A. Cieza
Institute for Astronomy, University of Hawaii, Honolulu, HI 96822, USA

Key Words .....

Abstract ....

CONTENTS

1 INTRODUCTION

Circumstellar disks are an inevitable consequence of angular momentum conservation during the formation of a star through gravitational collapse. Initially disks rapidly funnel material onto the star but, as the surrounding molecular core is used up or otherwise disperses, the accretion rate decreases and a small amount of material persists. That these disks can be considered protoplanetary is apparent not only through the geometry of the Solar System but also the large number and increasingly lower masses of known exoplanets.

Because disks exhibit a range of temperatures – hot near the star, cooler father away – they radiate strongly at a range of wavelengths from microns to millimeters. They can therefore be observed with infrared and radio telescopes and the mapping of wavelength to radius allows detailed models of their structure to be determined purely from unresolved photometry. Furthermore, their longevity, relative to the natal core, allows their properties to be studied in relation to the optically visible protostar.

Internal friction, or viscosity, within the disk drives continued accretion onto the star. To preserve angular momentum, the disk gradually spreads out with time. Its structure may also be strongly affected by photoevaporation, both from the central star and external stars, and the agglomeration of dust grains well beyond the typical sizes found in the interstellar medium including, ultimately, into planetesimals large enough to gravitationally perturb the disk. The various evolutionary pathways lead to inner holes and gaps that reveal themselves through a relative decrement in flux over a narrow range of wavelengths and which may also be imaged directly at sufficiently high resolution.

The Infrared Astronomical Satellite (*IRAS*) opened up the infrared sky and allowed the first statistical studies of disks to be made (Strom et al. 1989). Shortly thereafter the first sensitive detectors at millimeter wavelengths showed that many disks contained enough material to form planetary systems on the scale of our own (Beckwith et al. 1990). Interferometry at these long wavelengths provided the ability to resolve the disks and show that they really are flattened, rotating structures (Sargent & Beckwith 1987) but unequivocal evidence for their nature actually came in the optical, with the Hubble Space Telescope (*Hubble*), through exquisite images of disk shadows against a bright nebular background (O'Dell et al. 1994). The pace of discoveries has accelerated in the last decade due to increases in sensitivity, resolution, and wavelength coverage. The Infrared Space Observatory (*ISO*) and, in particular, the Spitzer Space Telescope (*Spitzer*)have greatly expanded the known disk inventory in terms of central stellar mass, age, environment, and evolutionary state. Interferometry has expanded to longer baselines and shorter wavelengths, including into the submillimeter

regime with the Submillimeter Array (*SMA*),providing the ability to map fainter structures in greater detail. The potential to address fundamental questions in protoplanetary disk studies provided significant motivation for the development of major new facilities including the Herschel Space Observatory (*Herschel*),and Atacama Large Millimeter Array (*ALMA*).

The rather short history of protoplanetary disk research may be followed in the regular Protostars and Planets series (Gehrels 1978; Black & Matthews 1985; Levy & Lunine 1993; Mannings et al. 2000; Reipurth et al. 2005). There are also several related reviews that have also been recently written for this series including the inner disk (Dullemond & Monnier 2010), debris disks (Wyatt 2008), and dynamical processes (Armitage 2011).

This review focuses on the properties and evolution of the outer parts of protoplanetary disks as determined principally from observations at mid-infrared to millimeter wavelengths. After briefly describing the classification of young stellar objects in §2, we begin by discussing the formation of disks in §3 and their basic properties when the central star first becomes optically revealed in §4. The second half concerns itself with the temporal properties of disks. We discuss their lifetimes in §5, the evidence for, and processes by which, disks evolve in §6, and the properties of disks transitioning into their end state in §7. Each section ends with a short bullet-point summary of the key points and these, in turn, are distilled into an overall summary in §8. There are many promising avenues for future exploration that new and planned facilities can address and we list those that we deem most exciting in §9.

2 CLASSIFICATION OF YOUNG STELLAR OBJECTS

The process of star and planet formation begins with the collapse of a molecular core. The mass is initially all in the core but it is processed through an accretion disk inwards onto the protostar and outwards through an outflow. Ultimately the core is dispersed and the remaining mass is concentrated in the star. There enough terminology associated with this process to form its own "diskionary" (Evans et al. 2009a) and many observational ways to characterize the progression. The most direct, that of measuring the mass in each component, is hard and more practical means are generally used, principally measuring disk accretion signatures in the optical or the distribution of warm circumstellar material in the infrared.

The infrared based classification dates back to Lada & Wilking (1984) who showed that Young Stellar Objects (YSO) in Ophiuchus formed 3 distinct groups based on whether the emitted energy was rising in the mid-infrared, declining but with a notable excess over the blackbody stellar photosphere, or with negligible infrared excess. This was formalized into 3 classes, I-II-III respectively, by Lada (1987) based on the slope of the spectral energy distribution (SED) between about 2 and 25 μm,

$$\alpha_{\rm IR} = \frac{d\log \nu F_\nu}{d\log \nu} = \frac{d\log \lambda F_\lambda}{d\log \lambda}. \quad (1)$$

Greene et al. (1994) subsequently introduced an additional refinement of "flat-spectrum sources", intermediate between Class I and II YSOs. The class sequence was shown to fit naturally into the theoretical framework of a rotating, collapsing core by Adams, Lada & Shu (1987). As the ability to detect faint millimeter emis-

sion improved, the categorization was extended to an earlier, Class 0, phase by Andre et al. (1993) and the decrease in circumstellar mass along the sequence was verified (Andre & Montmerle 1994). Table 1 summarizes the principal physical properties and observational characteristics for each class, where the numerical boundaries for $\alpha_{\rm IR}$ follow Greene et al. (1994).

A parallel accretion-based classification exists for the later optically visible phases: classical and weak-lined T Tauri stars. These correspond closely (though not exactly) to Class II and III YSOs respectively. Classical T Tauri stars have strong Hα and UV emission whereas weak-lined T Tauri stars show no or only very low indications of accretion. Historically the dividing line between the two was a uniform Hα equivalent width of 10Å but this has been refined to a stellar mass dependent limit to account for the lower continuum level in low mass stars (Barrado y Navascues & Martin 2003; White & Basri 2003).

Large *Spitzer* surveys have mapped about 90% of all the star forming regions within 1 kpc of the sun (e.g., Jorgensen et al. 2006; Harvey et al. 2006, 2007, Padgett et al 2008; Kirk et al. 2009; Rebull et al. 2006, 2010) and spectra have been obtained for over 2000 YSOs therein (e.g., Kesser-Silacci et al. 2006; Furlan et al. 2009; Oliveria et al. 2010). The precision and wavelength coverage of these observations show the tremendous diversity of disk SEDs and the inadequacy of a single parameter, $\alpha_{\rm IR}$, to characterize the full range, especially as disks dissipate and open up central holes. These so-called transition disks are the subject of §7. Cieza et al. (2007) introduced a two-parameter scheme to describe these based on the longest wavelength at which the observed flux is dominated by the stellar photosphere, $\lambda_{\rm turn-off}$, and the slope of the infrared excess, $\alpha_{\rm excess}$, computed from $\lambda_{\rm turn-off}$ to 24 μm. The census of Class III sources is highly incomplete in optical and infrared catalogs, however, because they lack strong accretion signatures and infrared excesses. Their youth is generally only betrayed through their location in the Hertzsprung-Russell diagram above the main sequence or by X-ray activity (Feigelson & Montmerle 1999).

A disk forms very early on and grows rapidly during the Class 0 collapse phase (see §3). On average, the embedded phases through Class I lasts for about ~ 0.5 Myr (Evans et al. 2009b). The properties of the disks as their central stars first become optically visible, i.e. Class II YSOs, are discussed in §4. The median disk lifetime after the embedded phase is about 2 Myr but the manner and the rate at which any individual star-disk system evolves varies greatly. These issues are discussed extensively in §§5, 6.

Protostellar outflows also exist during the disk accretion phase. They are highly collimated and powerful during the early Class 0 and I phases, but decline in strength and broaden as they evolve to Class II (Arce & Sargent 2006). Although they are not discussed further here, they present a potentially large source of confusion and must be kept in mind when interpreting disk observations, especially of younger systems.

It is also important to note that the SED classification does not give a unique description of the amount and distribution of circumstellar material. In particular, YSOs with disks along the line of sight will be highly extincted and can be mis-interpreted as more embedded, hence less evolved, objects. For example, a Class II YSO viewed at high inclination has a similar SED to a typical Class I YSO and an edge-on Class I YSO can have characteristics of a Class 0 YSO (Robitaille et al. 2006). Resolved images, ideally at multiple wavelengths, are required to fully characterize the evolutionary state of any individual YSO.

3 DISK FORMATION

3.1 Disk Formation During Core Collapse

The initial collapse of a molecular cloud core is onto a point source but a disk quickly forms as more distant material with higher angular momentum falls inward. The disk will extend out to the centrifugal radius, which is expected to grow rapidly with time, $R(t) \propto \Omega^2 t^3$, where Ω is the angular rotation rate of the core (Stahler et al. 1994). Disks should evolve rapidly, therefore, and their final size and mass will depend sensitively on the infall time (t^3) and the core properties (Ω^2). Basu (1998) notes that magnetized collapsing cores may not be in rigid rotation and that the radius may grow only linearly with time. Nevertheless, given the wide range of core rotation rates (Goodman 1993) and likely variation in infall duration, we should not be surprised by an inherent and large diversity in initial disk sizes and masses.

Hueso & Guillot (2005) model the formation and evolution of a protostar and accompanying disk in a collapsing molecular core. Within the first ~ 0.2 Myr the disk grows rapidly in size and mass and its surface becomes very hot due to infall of material from the core. As the core material is used up, the disk cools down and its mass decreases as it accretes onto the star.

Core collapse onto a disk will open up an approximately spherical cavity in the surrounding envelope of radius $R(t)$ that has been inferred from the presence of excess mid-infrared emission above that expected from a more extincted centrally peaked core (Jorgensen et al. 2005a; Enoch et al. 2009). Although there are many observations of inward motions on core size scales (e.g. Di Francesco et al. 2001), the direct detection of gas flow onto a disk has yet to be convincingly demonstrated. Chandler et al. (2005) find SO line absorption against the disk continuum in the IRAS 16293-2422B YSO but the spectral profile is approximately symmetric about the source velocity and cannot be clearly identified as pure infall. Watson et al. (2007) detect many mid-infrared lines of H_2O toward NGC1333-IRAS4B which they model as arising from a dense, warm, and compact region. They attribute this to shocked gas from an envelope onto a disk surface. However, Jorgensen & van Dishoeck (2010) mapped the 1.5 mm $3_{1,3} - 2_{2,0}$ transition of $H_2^{18}O$ from the ground and find the water emission is quiescent and follows the disk rotation.

Imaging embedded disks requires long wavelengths to see through the envelopes and arcsecond or higher resolution to match the disk sizes. Millimeter inteferometers meet these requirements and also filter out extended structures so that the emission from the compact disk dominates on long baselines, $\gtrsim 50\mathrm{k}\lambda$ (e.g, Keene & Masson 1990; Brown et al. 2000; Looney et al. 2000; Jorgensen et al. 2005b). A 1.1 mm continuum survey of 20 embedded YSO by Jorgensen et al. (2009) show that the disk flux is an average of four times higher in the embedded Class 0 phase than in Class I sources but, after allowing for higher temperatures due to greater accretion heating. the inferred disk masses show no significant dependence on evolutionary state. Masses in both Class 0 and I sources range from $\sim 0.02 - 0.1\,M_\odot$ with a median $0.04\,M_\odot$. This is quantitatively similar to the results from 2.7 mm observations of 6 sources by Looney et al. (2003)

The lack of dependence of disk mass on evolutionary state from Class 0 to Class I is contrary to expectations of steady disk growth as outlined above, whether the core is rigidly or differentially rotating. Rather, it indicates that disks form

quickly and that the flow of material from the envelope, which declines in mass by almost an order of magnitude between these two classes (Young et al. 2003), is rapidly transported through the disk.

One possibility for the rapid transport is disk instabilities. Laughlin & Bodenheimer (1994) first suggested that disks would be gravitationally unstable during the early formation stages due to the relatively high mass fraction in the disk versus that accreted onto the protostar. The instabilities would lead to sporadic bursts of high accretion and effectively self-regulate the disk mass from growing faster than the star (Vorobyov & Basu 2005, 2006; Vorobyov 2010). Many protostars have been observed to undergo short-lived bursts of activity due to high accretion and these events are named after the first such identified case, FU Orionis (Herbig 1977). Hartmann & Kenyon (1996) estimate that a typical low mass star may have an average of about 10 such outbursts during its formation.

Additional supporting observational evidence for "punctuated evolution" at these early stages is found in measurements of mass infall rates through the different components and the protostellar luminosity distribution. Eisner et al. (2005) find envelope infall rates are more than an order of magnitude higher than disk accretion rates rates in Class I YSO suggesting that mass builds up in the disk until a burst event occurs. It has long been known that Class I YSO are, on average, about an order of magnitude less luminous than expected for the steady release of gravitational energy as the envelope falls onto the protostar over the lifetime of the embedded phase (Kenyon et al 1990). Based on the statistics from the cores-to-disks *Spitzer* survey of 5 large, nearby molecular clouds, Evans et al. (2009b) concludes that, on average, a star gains half of its final mass in only $\sim 7\%$ of the ~ 0.5 Myr Class O plus I lifetime.

Some words of caution are necessary in the interpretation of these observations, however. The analyses of the continuum visibilities are based on rather sparse sampling of the Fourier plane and are subject to confusion with small scale infall shocks at the center of the envelope (Chiang et al. 2008). A more secure identification of an embedded disk requires spectral line observations showing rotation. The emission from the core and any protostellar outflow may still present significant confusion, although this is somewhat mitigated by observing species such as HCN and HCO^+ that only emit substantially in gas that is warmer and denser than the outer parts of the envelope. Recent work demonstrates the possibilities in this area with indications of Keplerian velocity profiles in moderately young, Class I sources (Brinch et al. 2007; Lommen et al. 2008; Jorgensen et al. 2009). More sensitive observations of optically thin isotopologues are required to discern disk kinematics from the core background in the younger, more embedded Class 0 phase. Such observations also have the potential to measure the central protostellar mass and track its growth against the evolution of the envelope and disk.

3.2 Continued Accretion from the Molecular Cloud

Although the surrounding molecular core disperses within about 0.5 Myr, the protostar and disk can remain embedded within their natal molecular cloud for much longer. For example, the $\sim$ 3 Myr old IC 348 cluster remains partially embedded in the Perseus molecular cloud (Tafalla et al. 2006). The longer timescale partially compensates for the lower density of the surroundings such that continued accretion from the large scale molecular cloud onto the disk may

be significant.

As a rough estimate, consider a relative speed between the YSO and cloud of $1\,\mathrm{km\,s^{-1}}$, and an average H_2 density of $100\,\mathrm{cm^{-3}}$. The YSO will capture all quiescent material within about 10^3 AU as it moves through the cloud and accumulates about $1\,M_{\mathrm{Jup}}$ over 3 Myr. The line of sight extinction toward the star is $A_V \sim 1$ mag and the average mass accretion rate over this time $\sim 3 \times 10^{-10}\,M_\odot\,\mathrm{yr^{-1}}$. Both are consistent with observations of evolved YSOs. With more careful modeling, but under more optimistic assumptions about the cloud density, Throop & Bally (2008) show that a YSO may accumulate as much as a MMSN as it orbits through a cluster forming molecular clump.

Circumstantial evidence for this scenario may be found in the observed dependence of the mass accretion rate on stellar mass, $\dot{M}_{\mathrm{acc}} \propto M_*^2$ (Muzzerolle et al. 2005), which is not well understood but agrees with the expectations of Bondi-Hoyle accretion (Padoan et al. 2005). There is little direct observational evidence, however, as studies have tended to focus either on the small scale of cores and disks or the large scale of molecular clouds with little linking the two.

In fact, both pointed single-dish and interferometric measurements of CO toward optically visible Class II YSOs show a high degree of cloud confusion (van Kempen et al. 2007; Andrews et al. 2010). Small maps of Taurus protostellar environments at moderate resolution show a complex structure with hints of filamentary connections linking disks and residual core material to the cloud, even for evolved Class III YSOs (Figure 1). The interplay between cloud and disk at Myr timescales is not well understood and deserves further study.

3.3 Section summary

4 PROPERTIES OF PROTOPLANETARY DISKS

The deeply embedded Class 0 and I phases of star formation only last for a small fraction of a disk lifetime, typically ~ 0.5 Myr compared to several Myr. By the end of the Class I phase the envelope has completely dispersed and the star formation process is effectively over. The disk now contains only a few percent of the central stellar mass and can be considered truly protoplanetary, not protostellar. Although there may be a small amount of accretion of material from the molecular cloud, the major elements governing the evolution of the disk at this stage are accretion onto the star, photo-evaporation from local or external radiation sources, agglomeration into larger bodies, and dynamical interactions with stellar or substellar companions.

Unless the disk is edge-on to our line of sight, the extinction to the central protostar is small and its spectral type can be determined through optical or near-infrared spectroscopy in most cases. The properties of the disk at this stage marks the baseline for studies of their evolution and for core accretion models of giant planet formation. In this section, we discuss the basic properties of the outer regions of protoplanetary disks around Class II YSO.

As a fiducial comparison, we use the Minimum Mass Solar Nebula (MMSN), the minimal properties of the primordial disk that formed the Solar System as inferred from scaling planetary compositions to cosmic abundances at each orbital radius (Kusaka et al 1970; Weidenschilling 1977). Because of the uncertainty in the composition of the giant planets, Weidenschilling (1977) quotes a range for the MMSN of $0.01 - 0.07\,M_\odot$. Here, we use the minimum of this range, $0.01\,M_\odot \approx 10\,M_{\rm Jup}$, as an absolute lower mass for the solar nebula out to the 30 AU orbit of Neptune. Extrasolar planetary systems have been found around 10% of Sun-like stars in the solar neighborhood and many planets detected to date are considerably more massive than Jupiter (Johnson 2009). The minimum mass disk required for their formation is proportionally higher.

The extrapolated surface density profile, which is an observable for resolved disks, has an approximate power law form, $\Sigma \propto r^{-3/2}$, although more sophisticated fits based on viscous disk evolution and planet migration models can be made (Davis 2005; Desch 2007).

The properties of the outer parts ($\gtrsim 1$ AU) of protoplanetary disks are mainly inferred from observations at mid-infrared through millimeter wavelengths although optical and near-infrared scattered light or silhouette observations can provide important information on disk radii and dust grain properties (Pinte et al. 2008; Throop et al. 2000).

4.1 Mass

Disk masses are best determined from (sub-)millimeter wavelength observations where the dust emission is optically thin except in the innermost regions where column densities are very high. The optical depth is the integral of the dust opacity, κ_ν, times the density, ρ, along the line of sight, $\tau_\nu = \int \rho \kappa_\nu ds = \kappa_\nu \Sigma$, where Σ is the projected surface density. A commonly used prescription for the dust opacity at millimeter wavelengths is

$$\kappa_\nu = 0.1 \left(\frac{\nu}{10^{12}\,{\rm Hz}} \right)^\beta \ {\rm cm^2\,g^{-1}} \tag{2}$$

(Beckwith et al. 1990). Both the absolute value and power law index, β, are related to the size distribution and composition of the dust grains (Ossenkopf & Henning 1994; Pollack et al. 1994). The normalization above also implicitly includes a gas-to-dust ratio of 100 and ρ, Σ refer to the total (gas plus dust) density. Dust accounts for 1% of the mass in the general interstellar medium but, as we discuss below, may evolve to a substantially higher fraction in disks. The corrective factor from dust to total mass is potentially a very large source of uncertainty.

For disks, $\beta \approx 1$ so $\kappa(1\,{\rm mm}) = 0.03$ cm^2 g^{-1} which implies $\tau(1\,{\rm mm}) = 1$ at a surface density $\Sigma \approx 30$ g cm^{-2}, corresponding to about 10 AU in the MMSN (Davis 2005) and an angular scale of $0\farcs07$ in the nearby Taurus star forming region. Protostellar disks are generally much larger than this and most of the resolved emission is indeed optically thin. On the other hand, the inner 10 AU likely constitutes a substantial fraction of the planet forming region of a disk. Not only high resolution but wavelengths longer than 1 mm are required to peer into this zone at the early phases of disk evolution.

For the general question of disk mass measurements on scales much larger than 10 AU, we can consider the emission to be optically thin and therefore directly

relate the observed flux, F_ν, to the mass,

$$M = \frac{F_\nu d^2}{\kappa_\nu B_\nu(T)}, \tag{3}$$

where d is the distance to the source. This shows an additional advantage of millimeter wavelengths in that the Planck function is close to the Rayleigh-Jeans regime, $B_\nu \approx 2\nu^2 kT/c^2$, and the emission is only linearly, rather than exponentially, dependent on the dust temperature.

The first large millimeter wavelength surveys to measure disk masses was carried out at 1.3 mm using a single element bolometer by Beckwith et al. (1990) in Taurus-Auriga and Andre & Montmerle (1994) in Ophiuchus. Using bolometer arrays, which provide better sky subtraction capability, hence lower noise levels and the ability to detect fainter targets, Andrews & Williams (2005, 2007b) augmented these surveys in size and expanded the wavelength coverage into the submillimeter regime with observations from 350 μm to 850 μm. The results of this work show that the masses of Class II YSO are lognormally distributed with mean $5 \times 10^{-3}\,M_\odot$ and standard deviation 0.7 dex. About one third exceed the MMSN. Both these regions are predominantly forming low mass stars, $M_* < 1\,M_\odot$ with spectral types K-M, and the mean ratio of disk to stellar mass is 0.9%.

By modeling the infrared-millimeter SED, Andrews & Williams (2005) showed that the simple mass derivation above is indeed reasonably accurate with a characteristic temperature, $T = 20$ K. This temperature is consistent with CO observations (Qi et al. 2004) and theoretical expectations (Chiang & Goldreich 1997). They also show that, for a 100 AU disk with the mass and surface density profile of the MMSN, about one third of the emission by mass is optically thick at 850 μm.

The biggest caveat to protoplanetary disk mass measurements at millimeter wavelengths is not uncertainties in the amount of optically thick emission, temperature, or even the gas-to-dust ratio but the hidden mass in large grains. Dust grows to much larger sizes in protoplanetary disks than in the interstellar medium and these "pebbles" or "snowballs" can hold considerable mass in a small solid angle with negligible effect on the SED. As a rule of thumb, observations at a wavelength λ only constrain the properties of dust grains out to a maximum size $a_{\rm max} \sim 3\lambda$ (Draine 2006). Few disks have only been detected beyond millimeter wavelengths and thus we know little about the general occurrence and distribution of centimeter and larger sized particles in disks. For a grain size distribution $n(a) \propto a^{-3.5}$ (Mathis, Rumpl, & Nordsieck), the total mass scales as $a_{\rm max}^{1/2}$ and substantial mass may be undetected. Detailed modeling by D'Alessio et al. (2001) show that the opacity prescription in equation 2 is valid for $a_{\rm max} \sim 0.3-3$ mm but is about a factor of 20 smaller for $a_{\rm max} = 1$ m implying correspondingly higher masses.

There is circumstantial evidence that disk masses have been substantially underestimated. First, the masses derived from (sub-)millimeter photometry are systematically lower than those estimated from accretion rates integrated over protostellar ages (Hartmann et al. 1998; Andrews & Williams 2007a). Second, these masses imply that only a few percent of circumstellar disks in nearby star-forming regions are massive enough to form giant planets, which is inconsistent with current statistics on the incidence of these planets in the solar neighborhood (Greaves et al. 2010). The observational evidence for grain growth from

sub-micron to millimeter and beyond sizes is discussed in §6.3.

4.2 Radius

Disk sizes are hard to measure because the outer parts are cool and emit weakly. They are still efficient absorbers, however, and images of disk silhouettes in Orion against the optically bright HII region background provide a simple and direct size determination. Vicente & Alves (2005) measure radii ranging from 50 to 194 AU for 22 Orion "proplyds" where the disk shadow can be clearly seen in *Hubble* optical images and an additional two outliers with radii of 338 and 621 AU. The latter object, cataloged as proplyd 114-426, is almost 3″ in angular extent, resolved in both radial and vertical dimensions, and provides perhaps the most famous disk image obtained to date (McCaughrean & O'Dell 1996; McCaughrean et al. 1998). Most of the Orion proplyds are apparent only through the photoevaporative flows from their surfaces, however, and Vicente & Alves (2005) estimate radii for 125 such objects from the size of the ionization front. Although there is substantial uncertainty associated in this indirect determination, they infer a median radius ~ 75 AU. They further note that the sample of *Hubble* proplyds accounts for only half the stars with known infrared excesses and suggest that over three quarters of the full sample of Orion disks have radii less than 75 AU.

Imaging disks at millimeter wavelengths requires inteferometry on account of their small angular scales in nearby star forming regions. A curious problem arose in that the size of the gas disk, as observed in rotational lines of CO, was found to significantly exceed the size of the continuum image (Pietu et al 2005; Isella et al. 2007). The differences could not be reconciled for a sharply truncated power law surface density profile (i.e., $\Sigma \propto R^{-p}$ for $R \leq R_{out}$, $\Sigma = 0$ for $R > R_{out}$) without introducing an arbitrary change in either the dust-to-gas ratio or dust opacity at the radius of the continuum disk. Similarly, McCaughrean & O'Dell (1996) found that pure power laws or sharp edges do not match the intensity profiles of Orion proplyd silhouettes and showed that an exponential decay at the outer boundary was required. Indeed physical models of viscous accretion disks (e.g., Lynden-Bell & Pringle 1974; Hartmann et al. 1998), predict an exponentially tapered profile of the form,

$$\Sigma(R) = (2-\gamma)\frac{M_d}{2\pi R_c^2}\left(\frac{R}{R_c}\right)^{-\gamma} \exp\left[-\left(\frac{R}{R_c}\right)^{2-\gamma}\right], \quad (4)$$

where M_d is the disk mass, R_c is a characteristic radius, and γ specifies the radial dependence of the disk viscosity, $\nu \propto R^{\gamma}$. Kitamura et al. (2002) first modeled millimeter wavelength disk images with this profile but their data were unable to differentiate between this and sharply truncated power law fits. With higher resolution observations, Hughes et al. (2008) showed that this prescription can naturally account for the apparent size discrepancy in millimeter imaging as the the optically thick CO line can be detected further out along the tapered edge than the optically thin dust continuum. It may also explain the smaller disk radii observed in CO isotopologues by Dartois et al. (2003).

R_c is a characteristic radius that delineates where the surface density profile begins to steepen significantly from a power law. As the disk does not have a sharp edge, a physical disk size must be specified in terms of an intensity threshold. A rough estimate of R_c may be obtained by noting that about 2/3 of the total disk mass (approximately flux) lies within it. More precisely, Hughes et al. (2008)

determine $R_c = 30 - 200\,\mathrm{AU}$ for four disks by fitting the profile in equation 4 to the continuum data. They compare with sharply truncated power law fits and find $R_{out} \approx 2R_c$. The tapered disks extend well beyond R_{out}, however, with midplane densities $n(\mathrm{H_2}) > 10^5\,\mathrm{cm^{-3}}$ for $R \lesssim 800\,\mathrm{AU}$.

By simultaneously fitting $850\,\mu$m interferometric visibilities (the Fourier transform of the sky brightness distribution) and infrared-millimeter SEDs Andrews et al. (2009, 2010) determine a wide range $R_c = 14 - 198\,\mathrm{AU}$ for 16 disks in Ophiuchus. Their sample is sufficiently large that they are able to identify a correlation with disk mass, $M_d \propto R_c^{1.6\pm0.3}$, which is likely to be a signature of disk formation physics rather than an evolutionary sequence. They do not find any correlation with the central star properties.

Isella et al. (2009) use the same density prescription to fit a sample of 11 disks mostly in Taurus-Auriga. They use a slightly different radial normalization which converts to a similar range, $R_c \simeq 30 - 230\,\mathrm{AU}$. In addition, Schaefer et al. (2009) compile radii for 16 disks around low mass stars in Taurus-Auriga based on sharply truncated power law fits to CO observations. Because of the different fitting technique, their values, $R_{out} \sim 100 - 1100\,\mathrm{AU}$, are not directly comparable with the above R_c measures but they similarly illustrate the large range of disk sizes and independence on stellar type.

The distribution of disk sizes can be related to the distribution of angular momenta of the initial cores. Isella et al. (2009) and Andrews et al. (2010) both conclude that the inferred range of angular momenta is about an order of magnitude lower than observed. The discrepancy either shows that most of the core's angular momentum is not transferred to the disk during its formation or that measurements of core angular momenta are overestimated in radial velocity measurements due to the inherent smoothing of turbulent fluctuations (Dib et al. 2010).

4.3 Structure

4.3.1 Surface density A resolved image of a disk at millimeter wavelengths provides not only a measure of its total mass and radius but also the distribution of mass, or surface density. Until recently this was characterized as a pure power law, $\Sigma \propto R^{-p}$, with values of p generally in the range $0 - 1$ (Mundy et al. 1996; Wilner et al. 2000; Lay et al. 1997; Kitamura et al. 2002; Andrews & Williams 2007a).

The exponential tapered fits of the form in equation 4 approximate a power law, $\Sigma \propto R^{-\gamma}$ for $R \ll R_c$, but the fitted values of $R_c \simeq 30 - 200\,\mathrm{AU}$ correspond to $\lesssim 1''$ in all but the closest disks and γ is actually determined largely from the steepness of the exponential taper. The Hughes et al. (2008) comparison of pure power law versus exponentially truncated power law fits shows similar indices but with slightly steeper pure power law fits due to the soft edge, $\langle p \rangle = 1.2, \langle \gamma \rangle = 0.9$ for four disks.

From larger samples, Andrews et al. (2009, 2010) finds a tight range consistent with all having the same value $\langle \gamma \rangle = 0.9$. Isella et al. (2009), on the other hand, find a very wide range $\gamma = -0.8$ to 0.8 with mean $\langle \gamma \rangle = 0.1$. Negative values correspond to decreasing surface densities for $R < R_c$ which may be an important signature of disk evolution (see §6). The discrepancy between these two teams may be related to the different fitting techniques or to the lower resolution and mass sensitivity of the Isella data. The low γ values in that work are found in

the smaller disks with $R_c < 100\,\mathrm{AU}$ which is below the $0\farcs7$ resolution of their 1.3 mm observations.

In general, all results agree that young protoplantary disks have flatter central density profiles than the canonical power law $p = 1.5$ MMSN (Weidenschilling 1977). There is even more uncertainty in the density profile of the MMSN than its mass, however, and an exponential tapered power law fit by Davis (2005) has $\gamma = 0.5$. The more relevant comparison is of absolute values in the planet forming zone. Andrews et al. (2009, 2010) infer surface densities, $\Sigma \approx 10 - 100\,\mathrm{g\,cm^{-2}}$ at 20 AU, in their sample of Ophiuchus disks that are in good agreement with the MMSN (Figure 2).

Whereas the disk-to-star mass ratio may be very high during the initial stages of formation (§3), the Toomre Q parameter, $Q(R) = c\Omega/\pi G\Sigma$ where c is the sound speed and Ω the orbital angular velocity (Toomre 1964), is generally much greater than unity for these Class II disks implying that they are gravitationally stable at all radii (Isella et al. 2009; Andrews et al. 2010). The one possible exception is DG Tau, a young protostar with by far the most massive disk in the two surveys.

The inferred surface densities are increasingly uncertain closer to the star due to the limited resolution of the observations, $\gtrsim 20\,\mathrm{AU}$, and also because the emission is becoming optically thick. As the discrepancy between Andrews et al. (2009, 2010) and Isella et al. (2009) shows, different data and fits extrapolate to very different surface densities at the $5-10\,\mathrm{AU}$ orbital radii of Jupiter and Saturn. This is not only a critical region for understanding planet formation but also for disk structure. The density is so high here that the midplane is shielded from radiation and cosmic rays. Unless radioactive elements are sufficiently abundant (Turner & Drake 2009), the ionization fraction may so low that matter is decoupled from the magnetic field and avoids the magneto-rotational instability (see §6.1). Current observations cannot address these issues and they will remain a challenge until the combined requirements of high sensitivity and high resolution at long wavelengths are met (Wilner 2004).

4.3.2 Scale height Protoplanetary disks are flared with a vertical scale height that increases with radius. Kenyon & Hartmann (1987) first suggested the possibility of flaring based on the large far infrared excesses detected by *IRAS* that could not be explained by a spatially flat disk. Direct evidence for flared disks can be found in the beautiful *Hubble* images of Taurus disk silhouettes against the scattered light of the central star (Burrows et al. 1996; Stapelfeldt et al. 1998; Padgett et al. 1999) and in Orion against the nebular background (Smith et al. 2005).

Characterizing the disk scale height is essential for modeling the thermal, ionization and chemical structure of disks and thence for interpreting atomic and molecular line observations. It is also important for understanding disk evolution as the outer parts, with their low densities and large scale heights, are particularly susceptible to photoevaporative losses.

For an azimuthally symmetric disk in hydrostatic equilibrium, the density is a function of both radius, R, and vertical height, Z,

$$\rho(R,Z) = \frac{\Sigma(R)}{\sqrt{2\pi}H}\,\exp\left(-\frac{Z^2}{2H^2}\right), \tag{5}$$

where $\Sigma(R)$ is defined in equation 4 and $H(R)$ is the scale height which depends

on the competition between thermal pressure and gravity, i.e., the temperature and surface density profiles of the disk. The temperature, in turn, depends on the amount of stellar radiation impacting the disk and therefore on its geometry. Chiang & Goldreich (1997) provide an elegant analytic solution to these coupled equations by approximating the radiative transfer with a hot surface layer that absorbs and reprocesses the starlight, which then heats a flared interior. They find an approximate power law dependence, $H \propto R^h$, with $h \approx 1.3 - 1.5$. D'Alessio et al. (1998) and Dullemond et al. (2002) iterate numerical solutions to the vertical disk structure and find similar results.

Observed disk SEDs have less mid-infrared emission than expected for this degree of flaring due to settling of dust grains toward the midplane (D'Alessio et al. 1999; Chiang et al. 2001). This flattening of the dust disk relative to the gas occurs very early in the evolution of a disk (Dullemond & Dominik 2004) and is discussed further in §6.

4.3.3 Velocity Disk masses at the Class II stage and beyond are a small fraction of the central stellar mass. Their motions are therefore expected to be Keplerian. Velocity profiles have been measured for only a handful of disks. The difficulty lies in finding disks that are sufficiently young and therefore bright enough to image in a spectral line, generally a millimeter wavelength rotational line of CO or isotopologue, yet not contaminated by emission from the residual envelope or neighboring cloud.

Koerner et al. (1993) resolved the ^{13}CO $J = 2 - 1$ line in the relatively large GM Aur disk and found the velocity profile was consistent with being Keplerian. Similarly, Dutrey et al. (1994) imaged the large circumbinary disk around GG Tau in ^{13}CO $J = 1 - 0$ and used a Keplerian velocity profile to determine a total stellar mass of $1.2\,M_\odot$. With improvements in instrumentation, leading to higher frequency and resolution observations, more studies followed shortly thereafter (e.g., Mannings et al. 1997; Duvert et al. 1998).

Guilloteau & Dutrey (1998) modeled the CO $J = 1 - 0$ channel maps (images at different velocities) of DM Tau to show that a Keplerian velocity profile was not only consistent but was the best fit. This was further exploited in the survey by Simon, Dutrey, & Guilloteau (2000) who determined dynamical masses for 9 systems and tested models of protostellar evolution. Schaefer et al. (2009) extended this work to later spectral types. As discussed in §3, Lommen and Brinch have used the same technique to derive protostellar masses at even earlier times during the earlier Class 0 and I stages.

Spectral line observations also determine disk inclinations to our line of sight with high accuracy (e.g., Qi et al. 2004; Raman et al. 2006, Isella et al. 2007), which is necessary for detailed modeling and characterization of other disk properties.

Many of the aforementioned studies also note that the line emission are well fit by only rotational plus thermal broadening. High spectral resolution observations of the TW Hydra and HD163296 disks by Hughes et al. (2011) show that the turbulent component is subsonic, $\leq 10\%$ and 40%, of the sound speed respectively at the ~ 100 AU scales of their observations. Such a low level of turbulent stirring provides ideal conditions for grain settling and growth, plantetesimal congregation, and protoplanetary accretion. Their data also show near-perfect Keplerian rotational profiles confirming that disk self-gravity does not appear to be significant in these objects (Figure 3).

4.3.4 Departures from azimuthal symmetry The discussion in this section has considered only the radial or vertical variation of disk properties on account of the dominant gravity of the central star. Azimuthal variations are of great interest, however, because they would signpost an additional influence, potentially disk self-gravity or proto-planets.

Disks are tiny compared to the distances between stars even in dense clusters and disruptive encounters are highly unlikely. For typical relative motions of $1\,\mathrm{km\ s^{-1}}$, the stellar density must be greater than $\sim 10^6\ \mathrm{stars\,pc^{-3}}$ for an encounter within 1000 AU of a disk within 1 Myr. Almost all disks that have been studied in detail are nearby and are either isolated or in low mass star forming regions where the stellar densities are orders of magnitude lower than this. Consequently, the likelihood that any azimuthal distortions in a young disk is due to an encounter with a nearby star is very low.

The surface density measurements described in §4.3.1 and Keplerian velocity profiles in §4.3.3 show that disk self-gravity is negligible by the Class II phase. As discussed in §3, however, younger disks in formation probably have much higher disk-to-star mass ratios. The disk around the partially embedded Herbig Ae star AB Aur may be an example of an unstable disk. Optical and near-infrared coronagraphic imaging by Grady et al. (1999) and Fukagawa et al. (2004) show spiral features in scattered light. Lower resolution millimeter interferometry confirms the larger scale asymmetries in the system (Corder et al. 2005) and deviations from Keplerian rotation that may indicate streaming motions along the arms or an unseen companion (Pietu et al. 2005; Lin et al. 2006; Figure 4).

The gravitational effect of planets on debris disks has been diagnosed in Fomalhaut (Chiang et al. 2009), postulated in β Pic (Mouillet et al. 1997), and suspected in others (Wyatt 2010 and references therein). Younger disks are further away and, the intriguing case of AB Aur notwithstanding, the resolution is not yet sufficient to search for such effects, although this is an exciting prospect for the future (Wolf & D'Angelo 2005; Narayanan et al. 2006).

4.4 Composition

4.4.1 Dust Dust dominates the opacity of protoplanetary disks and is the raw material for planetesimals. In the diffuse interstellar medium, dust is mainly composed of silicates with sizes $r \lesssim 0.1\,\mu$m with an admixture of graphite grains and polycyclic aromatic hydrocarbons (Draine 2003). During the passage through cold dark clouds to protoplanetary disks, molecules freeze out from the gas phase onto grain surfaces producing icy mantles (Bergin & Tafalla 2007; Pontoppidan et al. 2005) and grains collisionally agglomerate (Blum & Wurm 2008).

Silicates are readily identified through broad spectral bands at 10 and $18\,\mu$m (Henning 2010). Polycyclic aromatic hydrocarbons also have several mid-infrared features in this wavelength range (Tielens 2008). About 2000 protoplanetary disks were observed with the Spitzer Infrared Spectrometer (IRS) providing a wealth of information on the composition, size distribution, and evolution of the dust. We defer discussion to §6.3 and note here only that the dust in disks has been significantly processed via thermal annealing and agglomeration to have a much higher crystallinity fraction and larger sizes relative to the interstellar medium.

4.4.2 Gas Gas amounts to 99% of the total mass of the interstellar medium and the same is true, at least initially, for protoplanetary disks. Its detection,

however, presents a far tougher observational challenge than the minority dust component because it emits only at specific wavelengths and therefore requires high resolution spectroscopy.

Disk accretion, which can be measured through recombination line emission or excess hot continuum emission, provides unambiguous evidence for the presence of gas. However, the precise amount or physical conditions of the gas in the disk cannot be determined from these diagnostics (Hartmann 2009).

At the typical high densities and low temperatures of the bulk of a protoplanetary disk, the primary gaseous species is H_2. Fluorescent electronic transitions of H_2 in the UV arise from hot gas very close to the protostar (Herczeg et al. 2006). Near-infrared ro-vibrational lines also probe the inner disk, $\lesssim 1$ AU. Because the focus of this review is on the outer disk, we discuss mid-infrared observations of H_2 only and refer the reader to Najita et al. (2007) for details on the inner disk gas component.

As a symmetric molecule, H_2 has no electric dipole moment and only magnetic quadrupole transitions are permitted, i.e. $\Delta J = \pm 2$. These transitions are higher in energy and have lower spontaneous emission rates, thus weaker lines, than rotational lines of asymmetric molecules such as CO. Nevertheless, pure rotational lines of H_2 are accessible in the mid-infrared, with energies characteristic of the temperatures at several AU in a disk, a potentially very interesting regime for understanding giant planet formation. Bitner et al. (2007) detected and spectrally resolved 3 lines (H_2 S(1), S(2), S(4) corresponding to $J = 3-1, 4-2, 6-4$ respectively) in AB Aur. The linewidths locate the emitting region to 18 AU in radius but the rotational diagram indicates a temperature of 670 K, much hotter than the dust temperature at this radius. They infer that the gas is decoupled from the dust and excited by either protostellar UV or X-rays, or shocks from the infalling envelope (see also Bitner et al. 2008). Similarly, Martin-Zaidi ea (2007) detect the H_2 S(1) line in another intermediate mass Herbig Ae star, HD97048, and show that the high line-to-continuum ratio requires either an enhanced gas-to-dust ratio or an additional gas heating mechanism such as X-rays or shocks.

In both cases, the inferred gas mass is very small. For AB Aur where the multiple lines allow the level populations to be determined, $M_{H_2} = 0.5\,M_\oplus \simeq 0.1\%$ of the total disk mass. Effectively, only the top of the disk atmosphere is measured due to the high optical depth of the dust at these wavelengths. Based on the Chiang & Goldreich (1997) two-layer model, Carmona et al. (2008) calculate that mid-infrared H_2 detections require gas temperatures twice as high as the dust and a gas-to-dust ratio greater than 1000. This is possible through dust settling to the midplane but the low detection rates suggest that such extreme conditions are rare (Martin-Zaidi et al. 2010; Lahuis et al. 2007).

Trace amounts, $M_{HI} \sim 1\,M_\oplus$, of atomic hydrogen should also be present due to photodissociation of H_2 (Kamp et al. 2007). Although beyond the sensitivity of current instruments, it will be possible to detect the 21 cm line in many disks with the Square Kilometer Array (Kamp et al. 2008).

Fortunately, there are many other currently observable species present in disks from ionized and atomic at the disk surface to molecular deeper within. A surprising case is the optical line of [O I] at 6300 Å, which has been detected in the surface of strongly flared Herbig Ae/Be disks out to ~ 100 AU (Acke et al. 2005). Its origin is from the photodissociation of OH which results in excited neutral atomic oxygen. *Spitzer* spectroscopy has provided new and exciting results. [Ne II] is one of the more commonly seen lines (Pascucci et al. 2007; Lahuis et al.

2007) but its origin is unclear and may be due to protostellar outflows, at least for young disks (Pascucci & Sterzik 2009).

Ro-vibrational lines from the organic molecules, C_2H_2, HCN, and CO_2, have also been detected by IRS, in absorption through a nearly-edge on disk by Lahuis et al. (2006), and in emission by Carr & Najita (2008). Both studies conclude molecular excitation temperatures ranging from $300 - 700\,\mathrm{K}$ and a location in the inner $3 - 6\,\mathrm{AU}$ of the disks. The high abundances arise from a rich chemistry sustained by the sublimation of icy grain mantles in a warm molecular region above the disk midplane. Many more detections were made in the surveys by Pascucci et al. (2009) and Pontoppidan et al. (2010). Pascucci et al. (2009) extend the work to disks around lower mass stars and brown dwarfs and find a deficit of HCN which they attribute to a reduced photodissociation rate of N_2. Pontoppidan et al. (2010) extend the work to intermediate mass stars and find almost no molecular emission toward 25 Herbig Ae/Be stars (the exception being one CO_2 line). They suggest either photodissociation, lower gas-to-dust ratios, or masking by the strong continuum as the cause.

The bulk of the lines in the Carr & Najita (2008) IRS spectrum of AA Tau are rotational lines of OH and H_2O. These are important coolants and also of great astrobiological interest. Their model fits constrain the location of the emitting region to $\sim 2\,\mathrm{AU}$ radius and show high abundances that require vertical and potentially radial transport of ices from the inner, cooler regions of the disk. Salyk et al. (2008) found similar results toward an additional two disks and the large survey by Pontoppidan et al. (2010) show that these lines are common in T Tauri disks. The complex origin of the gas-phase water and its implications for understanding disk structure and evolution are discussed most recently by Meijerink et al. (2009) and Ciesla & Cuzzi (2006).

There are also many detectable molecular lines in the (sub-)millimeter wavelength regime. Observations of low energy rotational transitions, which can be excited even at the low temperatures and densities of the outer disk provide the best constraints on the total gas mass in a disk. CO lines are the strongest on account of its high abundance and large dipole moment. The dominant source of opacity in this case is not the dust but the lines themselves (Dutrey et al. 1997). Interferometric CO images therefore show the radial gas temperature gradient, $T \propto r^{-q}$, with values $q \simeq 0.4 - 0.7$ for both T Tauri and Herbig Ae/Be stars (Guilloteau & Dutrey 1998; Pietu, Dutrey & Guilloteau 2007) in agreement with the dust temperature derived from SED modeling (Andrews & Williams 2005). Multi-transition observations probe different $\tau = 1$ surfaces so provide information on the vertical temperature structure. Qi et al. (2006) show that the strong CO 6–5 emission of the TW Hydra disk requires a hot surface layer with a gas-dust temperature difference of up to 30 K that can be explained by X-ray heating. Observations of the rarer isotopologues, ^{13}CO and $C^{18}O$, probe deeper into the disk and show cooler midplane temperatures, $\sim 13\,\mathrm{K}$ (Dartois et al. 2003). CO condenses onto dust grains at about 20 K (Sandford & Allamandola 1993) and, indeed, by comparing with the dust continuum emission, Dartois et al. infer that the gas phase CO in the disk is depleted by about an order of magnitude. Similarly high depletions have been found in other T Tauri disks (e.g. Qi et al. 2004; Oberg et al. 2010). The situation is quite different for disks around the more luminous Herbig AeBe stars where the dust is warmer than the CO condensation temperature throughout. Within the uncertainties of CO isotopologue abundance and dust opacity, Pietu et al. (2005) and Panic et

al. (2008) show that the gas-to-dust ratios in the AB Aur and HD 169142 disks are consistent with the interstellar medium value of 100.

Rotational lines of other molecules further constrain the physical structure as well as the chemistry of the outer disk. The first results were obtained using singledish telescopes, measuring the globally averaged properties, and showed that other molecules including HCO^+ and H_2CO were also strongly depleted, as much as if not more than CO in classical T Tauri disks (Dutrey et al. 1997; van Zadelhoff et al. 2001; Thi et al. 2004). Photodissociated products such as CN were relatively abundant, however, which led to the picture of a photon dominated region at the surface of a warm intermediate layer with $T \sim 20-40\,\mathrm{K}$, $n(\mathrm{H_2}) \sim 10^6 - 10^8\,\mathrm{cm^{-3}}$, sitting on a cold, highly depleted midplane. Additional confirmation of a photon-dominated chemistry comes from CCH observations by Henning et al. (2010).

Thi et al. (2004) found a high deuterium fraction in TW Hydra, similar to values seen in dense cores and attributed to cool temperatures and high CO depletion (Caselli et al. 1999). Interferometric imaging resolves the D/H ratio, shows that it varies from ~ 0.01 to ~ 0.1 across the disk and peaks at $\sim 70\,\mathrm{AU}$ radius (Qi et al. 2008), a result with implications for understanding the high D/H ratio in comets and the delivery of water to Earth (Ehrenfreund & Charnley 2000). Figure 5 shows a suite of molecular line maps and shows directly the decrease in DCO^+ 3–2 intensity at the center of the disk where the higher temperatures lead to lower CO depletion. Deuterated species, in particular H_2D^+, and other molecules with very low condensation temperatures such as N_2H^+ should reveal the physical conditions and kinematics of the disk midplane in the outer disk. The lines are weak but have been detected in a small number of sources by Ceccarelli et al. (2004) and Dutrey et al. (2007) respectively. The cool temperatures of T Tauri star disks provide for a rich grain surface chemistry that is absent in warmer Herbig AeBe disks (Oberg et al. 2010). The reader is referred to Bergin (2009) for a more exhaustive discussion of disk chemistry.

The full analysis of the many species and lines now detected in protoplanetary disks requires sophisticated models to handle the physical, thermal, and chemical structure and the feedback of each of these on each other (e.g. Woitke et al. 2009). The complexity is such that, for T Tauri stars at least, there is no simple prescription for the gas mass. However, these observations provide substantial information about the disk structure and complement the broadband dust measurements. Disks have a dynamic atmosphere above a cool midplane: the temperature increases with height, the phase changes from molecular to atomic to ionized, and dust grains undergo sublimation and condensation of icy mantles as they move throughout.

Finally, as this review is being written, the first results are coming in from *Herschel* and its far-infrared spectrometers, PACS and HIFI. The [OI] $63\,\mu$m line is the strongest line in this regime and widely detected (Mathews et al. 2010). Combined with ground based CO measurements, it provides strong constraints on the gas mass (Thi et al. 2010). The lack of a clear detection of H_2O at submillimeter wavelengths with the HIFI spectrometer indicates that almost all the water is frozen onto icy mantles around large dust grains that have settled to the midplane (Bergin et al. 2010). In *Herschel*'s 3 year lifetime, we expect to learn much more about the gaseous content of disks in the giant planet forming zone.

4.4.3 Magnetic fields Magnetic fields are an energetically important constituent of the diffuse interstellar medium. Polarization measurements show magnetic field lines concentrating at the center of collapsing cloud cores in a classical "hour glass" configuration (Girart et al. 2006) but the role of magnetic fields in regulating the star formation rate remains controversial (Crutcher et al. 2009). Ambipolar diffusion increases the mass-to-flux ratio on smaller scales but some residual field must survive down to disk scales for the magneto-rotational instability, the only truly viable mechanism for disk viscosity, to exist. Singledish submillimeter measurements of polarization in disks (Tamura et al. 1999) have not been confirmed with interferometry (Hughes et al. 2009), however, and challenge theoretical understanding (Cho & Lazarian 2007).

4.5 Dependence on stellar mass

Disks are observed around a wide range of stars from very low mass to intermediate mass Herbig Ae/Be stars. Infrared excesses from disks around brown dwarfs are also detected at a similar frequency to stars (Luhman et al. 2005) and masses for a handful have been measured from millimeter wavelength measurements (Scholz et al. 2006). The different luminosities of the central object affect the disk chemistry as discussed above: disks around low mass stars lack nitrogen chemistry whereas disks around intermediate mass stars lack the CO condensation onto cold dust grains necessary for a diverse chemistry. The dependence of other fundamental properties such as the mass and structure can test theoretical models of disk formation and evolution.

Higher mass stars require more material to pass through a disk and we might therefore expect to see a positive correlation between disk mass and stellar mass (e.g., Natta PPIV). Figure 6 compiles (sub-)millimeter measurements of Class II disks from the literature and shows that there is a large scatter, ~ 0.5 dex, but confirms that disk masses tend to be lower around low mass stars such that the ratio, $M_d/M_* \sim 0.01$.

The relationship breaks down for the most massive stars. There is no (sub-)millimeter detection of a disk around an optically visible O star. The limits on the sensitive Orion proplyd survey provide the most stringent constraints to date,, $M_d/M_* \lesssim 10^{-4}$ for $M_* \geq 10\,M_\odot$ (Mann & Williams 2009a). This may be due to very short lifetimes (discussed further in §5) so that disks are not detectable by the time an O star is optically visible or, alternatively, massive stars may form without disks via the coalescence of lower mass stars. The situation is summarized in Zinnecker & Yorke (2007).

Disk size measurements, whether from optical observations of Orion proplyds (Vicente & Alves 2005) or millimeter visibilities of Ophiuchus disks (Andrews et al. 2009, 2010), are of a restricted range of stellar masses, $M_* \simeq 0.3 - 2\,M_\odot$ and do not follow a clear trend. Nevertheless, Andrews et al. (2010) do show a correlation between disk mass and radius and it therefore seems reasonable to extrapolate from the $M_d - M_*$ relation that the disks around higher mass stars should be larger.

Mid-infrared spectroscopy show that grain growth beyond micron sizes in disk surfaces is more efficient around low mass stars and the disks are flatter (Apai et al. 2005; Pascucci et al. 2009; Szucs et al. 2010). Yet the SED slope at sub-millimeter wavelengths, which is sensitive to the amount of millimeter sized grains throughout the disk, is not significantly different between Herbig AeBe

stars and T Tauri stars (Natta et al. 2004; Andrews & Williams 2005).

4.6 Section summary

5 DISK LIFETIMES

One of the most fundamental parameters on disk evolution studies is the lifetime of the disk itself, not only because it reflects the relevant time scale of the physical processes driving the dissipation of the disk, but also because it sets a limit on the time available for planet formation.

Even though the mass of the gas initially dominates that of the dust by two orders of magnitude in primordial disks, the dust is much easier to observe and thus most of the constraints on the lifetimes of circumstellar disks have been obtained by observing the thermal emission of the dust grains. These particles absorb stellar light and reradiate mostly in the $1\,\mu$m to 1 mm range. Since the temperature of the dust decreases with the distance from the central star, different wavelengths probe different disk radii (for a given stellar luminosity). In what follows, we summarize the observational constraints provided by near-infrared and mid-infrared observations, mostly from *Spitzer*, which has performed the most sensitive and comprehensive surveys of disks in star-forming regions to date. Towards the end of the section, we also briefly discuss current constraints on gas dispersal time scales.

5.1 Near-infrared results: the inner disk

Since there is a very well established correlation between the presence of near-infrared excess ($1 - 5\,\mu$m) and the occurrence of spectroscopic signatures of accretion (Hartigan et al. 1995), it is possible to investigate the lifetime of inner accretion disks ($R \lesssim 0.1$ AU) by studying the fraction of stars with near-infrared excess as a function of stellar age. Early studies of nearby star-forming regions found that $60-80\%$ of stars younger than 1 Myr present measurable near-infrared excesses, and that just $0 - 10\%$ of stars older than 10 Myr do so (e.g., Strom et al. 1989). Given the large uncertainties associated with model-derived stellar ages, it has been argued that individual star-forming regions lack the *intrinsic* age spread necessary to investigate disk lifetimes from individually derived ages and the apparent age dispersion is mostly driven by the observational uncertainties (Hartmann 2001). However, similar studies based on the disk frequencies in clusters with a range of *mean* ages (Haisch et al. 2001, Hillenbrand 2006) have led to essentially the same result: the frequency of inner accretion disks steadily decreases from < 1 to ~ 10 Myr.

The inner disk fractions observed in both young stellar clusters and in the distributed population of pre-main sequence stars in star-forming regions are consistent with mean disk lifetimes on the order of 2-3 Myr and a wide dispersion: some objects lose their inner disks at a very early age ($\lesssim 1$ Myr), even before they become optically revealed and can be accurately placed in the Hertzsprung-Russell diagram, while other objects retain their accretion disks for up to 10 Myr.

5.2 Spitzer results: the planet-forming regions of the disk

Since only circumstellar dust very close to the star ($R \lesssim 0.1$ AU) becomes hot enough to be detectable in the near-infrared, observations at these wavelengths provide no information on the presence of circumstellar material beyond ~ 0.5 AU. As a result, disk lifetime studies based on near-infrared excesses always left room for the possibility that stars without near-infrared excess had longer-lived outer disks with enough material to form planets at radii not probed by these short wavelengths.

IRAS and *ISO* both had the appropriate wavelength range to probe the planet-forming regions of the disk ($R \sim 0.5 - 20$ AU) but lacked the sensitivity needed to detect all but the strongest mid- and far-infrared excesses in low-mass stars at the distances of the nearest star-forming regions. During its 6-year cryogenic mission, *Spitzer* provided, for the first time, the wavelength coverage and the sensitivity needed to detect very small amounts of dust in the planet-forming regions of thousands of YSOs. The wealth of data made available by *Spitzer* has not only firmly established the dissipation time scale of primordial disks, but also made it possible to address second-order questions such as the effect of stellar mass, multiplicity, and external environment on disk lifetimes.

5.2.1 Stellar clusters and associations

Just as was done for the inner disk with near-infrared studies, the dissipation time scale of regions farther out in the disk can be investigated by observing the fraction of stars that show mid-infrared excesses in clusters of different ages. Reaching the stellar photospheres of all the targets is needed to unambiguously establish the fraction of them that have an infrared excess indicating the presence of a disk. However, while at 8.0 μm *Spitzer* was able to detect the stellar photospheres of solar-type stars at distances of up to 1 kpc, at longer wavelengths it was only sensitive enough to detect solar-type photospheres within ~ 200 pc. Since there are very few stellar clusters within 200 pc, we focus on the results from IRAC (3.6 to 8.0 μm) observations.

Comparing the disk fractions of stellar clusters presented by different *Spitzer* studies is not completely straightforward as the methods used to decide which objects are members of the cluster, the disk identification criteria, sensitivities, and ranges of stellar masses considered vary from study to study. With these caveats in mind, we summarize the results of IRAC studies of solar-mass stars of young stellar clusters and associations.

Very young embedded clusters (age ≤ 1 Myr) such as Serpens and NGC 1333 show disk fractions of the order of 70 to 80% (Winston et al. 2007; Guthermuth et al. 2008). This implies that pre-main sequence stars without a disk, showing photospheric IRAC fluxes, are seen even in extremely young star-forming regions. Clusters in the $2 - 3$ Myr range, such as IC 348 and NGC 2264, show IRAC disk fractions of the order of 40 to 50% (Lada et al. 2006, Sung et al. 2009), while regions with estimated ages around ~ 5 Myr, such as Upper Scorpius and NGC 2362 exhibit disk fractions that are already below 20%. By $\sim 8 - 10$ Myr old, primordial disks with IRAC excesses become exceedingly rare as attested by their very low incidence ($\lesssim 5\%$) in regions such as the TW Hydra, σ Ori, and NGC 7160 associations (Sicilia-Aguilar et. 2006; Hernandez et al. 2007).

The main results on disk lifetimes from IRAC studies of young stellar clusters listed above are indistinguishable from those obtained by pre-*Spitzer* near-infrared studies. This is not too surprising considering that IRAC wavelengths only trace regions inward of ~ 5 AU around solar type stars. These regions are

further out in the disk than those traced by near-infrared observations, but still exclude the bulk of the disk material. Thus, the question remains: can *primordial* outer disks ($R > 5\,\mathrm{AU}$) survive beyond 10 Myr? To address this question, we must turn to the longer wavelength camera, MIPS, on *Spitzer*, and studies of star-forming regions within 200 pc, where 24 μm observations are sensitive enough to reach the stellar photosphere of their targets and unambiguously identify the presence of a disk.

5.2.2 The distributed population of pre-main sequence stars Firmly establishing the longevity of primordial disks was one of the central goals of two *Spitzer* Legacy Programs: "From Molecular Cores to Planet-forming Disks" (c2d, Evans et al. 2003) and "Formation and Evolution of Planetary Systems" (FEPS, Meyer et al. 2003).

As part of the c2d project, *Spitzer* observed over 150 WTTSs associated with the Chameleon, Lupus, Ophiuchus, and Taurus star-forming regions, all within 200 pc of the sun. As one the main goals was to establish whether the outer disk could significantly outlive the inner disk, the c2d sample of WTTSs was mostly composed of X-ray identified and spectroscopically confirmed pre-main sequence stars *without* evidence for an inner accretion disk.

Results from the c2d project (Padgett et al. 2006; Cieza et al. 2007, Wahhaj et al. 2010) show that $\sim 80\%$ of young WTTSs present 24 μm fluxes consistent with bare stellar photospheres. Since 24 μm observations are sensitive to very small amounts of micron sized dust ($\ll 1\,M_\oplus$) out to tens of AU from the central star, this suggests that once accretion stops and the inner disk dissipates, the entire disk goes away very quickly. The fraction of c2d WTTSs with 24 μm excesses is a function of stellar age. Approximately 50% of the WTTSs younger than $\lesssim 1 - 2\,\mathrm{Myr}$ do not have a disk, suggesting that a significant fraction of the entire pre-main sequence population lose their disks by an age of $\sim 1\,\mathrm{Myr}$. On the other hand, none of the WTTSs in the c2d sample older than $\sim 10\,\mathrm{Myr}$ has a detectable disk. Also, many of the WTTS disks have very low fractional disk luminosities, ($L_{\mathrm{disk}}/L_* < 10^{-3}$), and are thus more consistent with optically thin debris disks than with primordial disks.

Very similar results were obtained by the FEPS project, which observed 314 solar-type stars with a median distance of 50 pc and ages ranging from 3 Myr to 3 Gyr. The youngest age bin in the FEPS study included 34 targets younger than 10 Myr and a mean age of $\sim 5\,\mathrm{Myr}$. They find that only 4 out of those 34 targets had optically thick primordial disks, while 5 of them had optically thin debris disks. The second youngest bin in their study had 49 targets with estimated ages in the 10 to 30 Myr range. In this age bin, they identified 9 debris disk and only one primordial disk (Carpenter et al. 2009). The only target with a primordial disk in this age range was PDS 66, a member of the Lower Centaurus Crux association with an *estimated* age around 12 Myr (Preibisch & Mamajek 2008).

Both the c2d and FEPS results strongly suggest that, while there is a wide dispersion on disk lifetimes, $\sim 10\,\mathrm{Myr}$ is a firm upper limit for the longevity of primordial circumstellar disks around solar-type stars. The very high dust mass sensitivity of their observations implies that forming planets must have built most of their mass within 10 Myr of the formation of the star. They also show that there is a significant overlap in the age distributions of primordial and debris disks. Exactly how and when primordial disks evolve into debris remains an

open question and will be discussed in §6.4.

5.3 Dissipation timescale

The fact that very few objects lacking near-infrared excess show mid-infrared excess emission implies that, once accretion stops and the inner disk clears out, the entire disk dissipates very rapidly. This is also supported by (sub-)millimeter observations (Andre & Montmerle 1994; Andrews & Williams, 2005, 2007) showing a very strong correlation between the detectability of a disk at these long wavelengths and presence of an inner accretion disk. This implies that the vast majority of pre-main sequence stars in any given population are either accreting CTTSs with excess emission extending all the way from the near-infrared to the sub-millimeter or have bare stellar photospheres. Based on the small incidence of objects lacking an inner disk that have evidence for an outer disk, the dissipation timescale of the entire primordial disk once accretion stops has repeatedly been estimated to be $\lesssim 0.5\,$Myr (e.g., Skrutskie et al. 1990; Wolk & Walter 1996; Cieza et al. 2007). This finding, that circumstellar material can survive at all radii ($R \lesssim 0.1 - 200\,$AU) for several Myr, while later the dissipation of the entire disk occurs in a much shorter timescale is known as the "two-time-scale" problem. Disk evolution models combining viscous accretion with photoevaporation (e.g., Alexander et al. 2006a,b) have successfully been able to reproduce this behavior (see §6.2).

5.4 Dependence on stellar mass

Young stellar clusters and associations provide an excellent opportunity to investigate disk lifetimes as a function of stellar mass as they contain large samples of mostly coeval stars spanning a large range of stellar masses. In their study of the 5 Myr old Upper Scorpius OB association, Carpenter et al. (2006) obtained 4.5, 8.0 and 16 μm photometry of 204 members with masses ranging from ~ 0.1 to $20\,M_{\odot}$. They find that while $\sim 20\%$ of their 127 K and M-type targets (masses $\sim 0.1 - 1.2\,M_{\odot}$) are surrounded by optically thick, primordial circumstellar disks, none of their 30 F and G-type stars (masses $\sim 1.2 - 1.8\,M_{\odot}$) had any evidence for a disk at wavelengths $\leq 16\,\mu$m.

An almost identical result was obtained by Dahm & Hillenbrand (2007) in the also 5 Myr old cluster NGC 2362. They found a total IRAC disk fraction of $\sim 20\%$ (7% of strong excesses and 12% of weaker excesses) among 220 stars with estimated masses below $1.2\,M_{\odot}$ and a complete absence of IRAC excesses among 33 stars with estimated masses above $1.2\,M_{\odot}$. MIPS observations of NGC 2362 (Currie et al. 2009) and other 5 Myr old clusters such as λ Orionis (Hernandez et al. 2009) do show 24 μm excesses for objects with masses above $1.2\,M_{\odot}$, but they are all consistent with the optically thin emission expected from debris disks. Overall, the *Spitzer* results suggest that, while primordial circumstellar disks can last for up to 10 Myr around solar and lower-mass stars, disk lifetimes are a factor of ~ 2 shorter around higher mass objects. The higher accretion rates and radiation environment are likely to be responsible for the shorter disk lifetimes in higher mass stars (Hillenbrand 2008; Calvet et al. 2005, Garcia Lopez et al. 2006).

At the lower end of the mass distribution, the statistics are much poorer. The disk fractions of brown dwarfs in relatively young regions (age $1 - 3\,$Myr) such

as Taurus, Chamaeleon I, and IC 348 has been found to be between 40 and 50% with statistical uncertainties as large as 10 to 20% (Luhman et al. 2005, Guieu et al. 2007, Monin et al. 2010). For the 5 Myr Upper Scorpius region, the reported values range from $37 \pm 9\%$ (Scholz et al. 2007) to $11^{+9}_{-3.3}\%$ (Riaz et a. 2009). Also, 3 of the 5 known brown dwarfs in the 10 Myr old TW Hydrae association have infrared excesses indicating the presence of a disk (Riaz & Gizis 2008). Taken together, these observations suggest that the dissipation time scales of disks around substellar objects are *at least* as long as those of solar-mass stars, although significantly longer disk lifetimes cannot be ruled out based on the available data.

5.5 Gas dispersal

Studies of gas dispersal lag behind those of the dissipation of the dust. Directly probing the bulk of the gas (e.g., H_2) in a large number of primordial disks still remains beyond current observational capabilities (Martin-Zaidi et al. 2010). Even though tracers of cold and warm gas, such as millimeter and infrared lines of CO have been observed in a number of objects (Schaefer et al. 2003; Najita et al. 2003; Dent et al. 2005; Brittain et al. 2007; Salyk et al. 2009), the presence of gas as a function of stellar age has most systematically been studied by observing accretion indicators.

Using the equivalent widths and velocity profiles of the Hα line to identify accretors, Fedele et al. (2010) recently studied the fractions of accreting objects in stellar clusters with ages in the $1-50$ Myr range. They find no accreting objects in the clusters older than 10 Myr down to an accretion sensitivity estimated to be $\sim 10^{-11}\,M_\odot\,\mathrm{yr}^{-1}$. They also find that, in most clusters, the fraction of accreting stars is systematically lower than the fraction of objects with *Spitzer* excesses in IRAC bands. This is expected as $\sim 20\%$ of non-accreting pre-main sequence stars (i.e., WTTSs) have IRAC excesses (Cieza et al. 2007; Damjanov et et. 2007; Wahhaj et al. 2010), while the fraction of accreting pre-main sequence stars (i.e., CTTSs) lacking IRAC excesses is significantly smaller, of the order of $\lesssim$ 2-5% (e.g., Cieza et al. 2010, Muzerolle et al. 2010).

Accretion only probes the presence of gas in the inner accretion disk. Consequently, our current understanding of the time scale of the gas dispersal is in an analogous situation to that of the dust dissipation prior to *Spitzer*: although the longevity of gaseous inner disks is well established to be $\lesssim 10$ Myr, the possibility of significant amounts gas remaining for longer period of times at larger radii still exists. However, according to the "UV-switch" model (Alexander et al., 2006), photoevaporation will remove all circumstellar gas very quickly ($\ll 1$ Myr) once accretion stops (see §6.2). *Herschel* studies currently underway of sensitive gas tracers, such as the 63.2 μm [O I] line, should be able to test this prediction.

5.6 Environmental influences

Protoplanetary disks are detected in a range of environments from low mass, sparsely populated molecular clouds to massive, dense stellar clusters. In nearby, well studied, low mass star forming regions, there is a remarkable similarity in the average disk properties from region to region as demonstrated from mid-infrared colors (Fang et al. 2009) and spectra (Furlan et al. 2008) and also in their mass distributions and sub-millimeter colors (Andrews & Williams 2005, 2007).

This is not surprising given that disk sizes are orders of magnitude smaller than typical star-to-star distances except perhaps in the densest parts of very young protoclusters and disruptive encounters with a passing star is not a common evolutionary determinant (Scally & Clarke 2001). Gravitational perturbations have a strong impact on disk evolution, however, in close binary or multiple systems.

The median disk lifetime of ~ 3 Myr discussed in §5 is derived from surveys of many clusters. There is a rather small dispersion in the disk fraction at any given age despite the different cluster sizes and whether or not they contain massive stars. These mid-infrared observations are unable to measure the properties of the outer parts of the disk, however, which are more susceptible to external influences.

5.6.1 Dynamical Disruption in Binaries About half of field stars are in binary or higher order multiple systems (Deepak et al. 2010). For unknown reasons, the binary fraction is about two times higher in the young Taurus-Auriga molecular star forming region (Mathieu et al. 2000), where a large number of detailed disk studies have been made. The orbital resonances in these systems have a profound influence on disk evolution. Artymowicz & Lubow (1994) show that (coplanar) disks around each star in a binary system will be truncated at the outer edge and a circumbinary ring about both stars will be truncated at the inner edge. As a rough guide for near circular orbits with semi-major axis a, the circumprimary disk is limited in size to $\sim a/2$ and the circumbinary disk's inner edge is $\sim 2a$. Higher eccentricities lead to greater disk erosion.

There are a few resolved disk images that confirm this general pattern. GG Tau is is one of the largest and perhaps best studied circumbinary disks with an inner radius of 180 AU (Guilloteau, Dutrey & Simon 1999) although it appears to be bigger than expected given the $a = 32$ AU, $e = 0.34$ binary orbit (Beust & Dutrey 2005). UY Aur (Duvert et al 1998) and CoKu Tau 4 (Ireland & Kraus 2008) are additional examples of massive circumbinary disks but they appear to be rare exceptions rather than the rule. Outwardly truncated circumstellar disks, only few tens of AU in diameter, have also been detected in binary systems, L1551-IRS5 (Rodriguez et al. 1998), GQ Lup (Dai et al. 2010), HD 98800 and Hen 3-600 (Andrews et al. 2010).

High resolution speckle imaging studies searching for a connection between binaries and premature disk dissipation initially yielded mixed and inconclusive results. Ghez et al. (1993) surveyed ~ 70 pre-main sequence stars in Taurus and Ophiuchus and concluded that the incidence of close binaries ($a < 50$ AU) in WTTS is enhanced with respect to that of CTTS. This was not confirmed, however, by subsequent larger studies in Taurus (Leinert et al. 1993; Kohler & Leinert 1998). Yet a survey of ~ 160 pre-main sequence stars in Ophiuchus by Ratzka et al. (2005) showed that YSOs with infrared excesses tend to have fewer companions and at smaller projected separations than diskless YSOs.

Here, again, the uniformity and sensitivity of *Spitzer* studies has improved our understanding of the situation. Cieza et al. (2009) combined the results from several multiplicity surveys of pre-main sequence stars with *Spitzer* data of four star-forming regions and showed that the distribution of projected separations of systems with mid-infrared excesses are in fact significantly different from that of systems without. Binaries with projected separations less than 40 AU are half as likely to possess a disk than those with projected separations in the $40 - 400$ AU

range. Duchene et al. (2010) find a similar result with a somewhat smaller sample. (Sub-)millimeter fluxes are also known to be lower for similarly close binaries indicating that the bulk of the disk has been lost (Osterloh & Beckwith 1995; Jensen et al. 1994, 1996; Andrews & Williams 2005).

Even though several factors (e.g., the incompleteness of the census of close binaries, the use of unresolved disk indicators, and projection effects) tend to weaken its observable signature, the effect of multiplicity on disk lifetimes could be very strong. The distribution of physical separations, a, in solar-type pre-main sequence binaries is expected to peak around 30 AU as in field stars (Duquennoy & Mayor 1991; Deepak et al. 2010). The disks around most binary systems hence should have truncation radii of the order of $(0.3-0.5)a \sim 10-15\,\mathrm{AU}$ (Papaloizou & Pringle 1977). These truncation radii are about an order of magnitude smaller than the typical radii of disks around single stars (see §4.2). For an accretion disk with $\gamma = 1$ (see §4.3.1), the viscous time scales linearly with radius and is therefore also about an order of magnitude smaller. This implies that the lifetimes of disks around the individual components of most binary systems should be $\sim 10\%$ of those of single stars or about 0.3 Myr. These very short lifetimes for the stars in medium-separation binary systems may explain both the presence of very young diskless stars and the large dispersion in disk dissipation time scales.

5.6.2 Photoevaporation by Massive Stars Most stars form in large clusters with hundreds if not thousands of stars (McKee & Williams 1997; Lada & Lada 2003). Such large stellar groups are highly likely to contain an O star which bathes neighboring stars and their disks in a UV radiation field that may be several orders of magnitude above the Habing interstellar average. The effect is to rapidly erode the more loosely bound outer parts of a disk.

Hubble observations of photoevaporating protoplanetary disks, dubbed "proplyds", in the Orion trapezium cluster (O'Dell et al. 1993; O'Dell & Wen, 1994) provided not only the first direct images of circumstellar disks, but also dramatic evidence of the strong effect external radiation fields can have on their outer regions. Very Large Array (*VLA*) observations of bremsstrahlung radiation from the ionized gas escaping from the disks implied sufficiently high mass loss rates, $\dot{M} \sim 10^{-7}\,M_\odot\,\mathrm{yr}^{-1}$ (Churchwell et al. 1987; Zapata et al. 2004), to cause the loss of a MMSN in 0.1 Myr. The spectacular *Hubble* images of photoevaporating disks embedded in small ionized cocoons make a stunning contrast to the large Taurus disks in their more benign low radiation environment (Padgett et al. 1999). The pictures are somewhat misleading, however, in that the central regions of Orion disks are not strongly affected. Except for disks very close to the O stars where ionizing photons directly impinge on the disk surface, the disk develops a thick photon dominated region with a temperature $\sim 10^3$ K. The corresponding thermal velocity, $\sim 3\,\mathrm{km\,s}^{-1}$, is bound to the central star for radii $\lesssim 100\,\mathrm{AU}$ (Adams et al. 2004). Gas pressure can cause mass loss at smaller radii but the evaporation timescale within solar system scales, $< 50\,\mathrm{AU}$, is tens of Myr (Clarke 2007).

Measurements of Orion disk masses bear this out. The strong bremsstrahlung emission necessitates observations at sub-millimeter wavelengths where the dust emission dominates and show a handful of disks with masses exceeding a MMSN at the center of the Trapezium cluster (Williams, Andrews, & Wilner 2005). Compared with Taurus and Ophiuchus, however, the disk mass distribution is truncated at the upper end. No disks more massive than $34\,M_{\mathrm{Jup}}$ exist within

the central 0.3 pc (Mann & Williams 2009a). The most massive disks are likely to be the largest and therefore the most susceptible to photoevaporation. The discrepancy in mass is roughly consistent with the smaller median size of Orion proplyds compared to Taurus disks (§4.2). Assuming a R^{-1} surface density profile, however, the fraction of disks with at least a MMSN, $10\,M_{\rm Jup}$, within 60 AU is similar, $\sim 11-13\%$, in Taurus, Ophiuchus, and Orion and, incidentally, comparable to the detection rate of Jupiter mass extrasolar planets.

There are more massive disks further away from the center of the Trapezium Cluster, including a $66\,M_{\rm Jup}$ disk in a wide binary system (Mann & Williams 2009b). The factor of almost two in mass between the most massive disks in and out of the cluster center is hard to explain via dynamical interactions (Olczak et al. 2006) and essentially confirms that photoevaporation is the cause of the relatively low masses at the center. From the full *SMA* 880 μm survey, Mann & Williams (2010) find that the maximum disk mass steadily increases with distance from the O6 star, θ^1 Ori C, and that the mass distributions are their most different at a dividing line of 0.3 pc radius.

VLA and *SMA* observations do not currently have sufficient sensitivity to study more distant regions. However, *Hubble* and *Spitzer* observations find similar morphological features to the Orion proplyds in other massive star forming regions (Smith et al. 2003; Balog et al 2006). Hernandez et al. (2008) find that the γ Velorum cluster has a low fraction of sources with infrared excesses for its age and consider disk photoevaporation as a possibility but also note the uncertainty in the cluster age. The disk fraction decreases by about a factor of 2 within the central 0.5 pc of the Rosette nebula (Balog et al. 2007) and the central 1 pc of S Monoceros (Sung et al. 2009) but the statistics are limited by small numbers. External evaporation can only remove the inner disk on such short timescales with very strong radiation fields that ionize the disk and boil it off at $\sim 10^4$ K (Adams et al. 2004; Clarke 2007). It is hard to reconcile this with the parsec-scale sphere of influence of a massive star unless the stellar orbits are highly eccentric (Storzer & Hollenbach 1999).

Balog et al. (2008) show that the Spitzer 24 μm dusty tails in these regions are not detected in Paα and are effectively gas free. They suggest that photoevaporation removes the gas very quickly but that a dusty reservoir is replenished by the collisions of large bodies left behind in the disk. Throop & Bally (2005) consider the rapid enhancement of the dust-to-gas ratio in photoevaporating disks as a potential trigger for planetesimal formation. External evaporation has also been considered as a possible explanation of the steep drop in the surface density of Kuiper Belt Objects beyond 50 AU (Jewitt, Luu, & Trujillo 1998).

5.6.3 The effect of metallicity The effect of the metallicity, or the intial dust-to-gas content, on the evolution of protoplanetary disks has not been well studied, at least at the early stages. It is known that the metallicity of the host star is strongly correlated with the presence of hot Jupiters (Fisher & Valenti 2005). This may be due to an enhanced rate of planetesimal formation (Johanssen et al. 2009) but longer disk lifetimes may also play a role. In a small sample, d'Orazi et al. (2009) do not find any significant difference in the metallicities of Taurus and Orion WTTS or CTTS. On the other hand, Yasui et al. (2009) showed the the inner disk fraction, as measured by near-infrared excesses, is significantly smaller in low metallicity clusters at the edge of the Galaxy. This is in accord with photoevaporative models of disk evolution (Ercolano & Clarke

2010).

5.7 Section summary

- Circumstellar disks have a median disk lifetime of $\sim 3\,\mathrm{Myr}$ with a large dispersion ($< 1 - 10\,\mathrm{Myr}$).
- Circumstellar disks dissipate faster around high-mass stars than around solar-type stars.
- Very low mass-stars and brown dwarfs have disk lifetimes that are *at least* as long as those of solar-type stars.
- Medium separation binaries ($R \sim 5 - 100\,\mathrm{AU}$) significantly reduce disk lifetimes.
- High radiation environments erode the outer parts of disks but leave their interiors intact.
- Planets must built most of their mass within 10 Myr of the formation of the star.

6 DISK EVOLUTION

Understanding the physical processes that drive the evolution of primordial circumstellar disks, as they evolve from optically thick to optically thin, is crucial for our understanding of planet formation. Disks evolve through various processes, including viscous accretion, dust settling and coagulation, dynamical interactions with (sub-)stellar companions and forming planets, and photo-evaporation by FUV, EUV, and X-ray radiation. In this section we summarize the models and observational constraints for the different processes that control the evolution of primordial circumstellar disks.

6.1 Viscous accretion

To first order, the evolution of primordial disks is driven by viscous accretion. The observational evidence for accretion in young stellar objects is robust and includes the observed ultraviolet and optical continuum excesses (e.g., Bertout, Basri, & Bouvier 1988; Hartigan et al. 1990; Konigl 1991; Valenti, Basri, & Johns 1993; Calvet & Gullbring 1998) and the emission line profiles of many optical and near-infrared features (Edwards et al. 1994; Hartmann, Hewett, & Calvet 1994; Muzerolle et al. 2001). The accretion from the inner disk onto the star is relatively well understood and well constrained observationally. The large velocity widths, intensities, and profiles of emission lines such as Hα, Brγ and Ca II can be successfully reproduced by magnetospheric accretion models (Muzzerolle et al. 1998a,b). Accretion across the disk however, can not be directly observed and the physics driving this process still remains to be established.

Circumstellar material can only be accreted onto the star if it loses angular momentum. Conservation of angular momentum then implies that, while most of the mass in the disk moves inward, some material should move outward, increasing the size of the initial disk. The source of the viscosity required for disk accretion and the mechanism by which angular momentum is transported remains a matter of intense debate. For this reason, most viscous evolution models still

describe viscosity, ν, using the α parameterization first introduced by Shakura & Sunyaev (1973), according to which $\nu = \alpha H_P C_S$, where H_P is the pressure scale height of the disk and C_S is the isothermal sound speed. H_p and C_S provide upper limits for the mixing length of the gas and its turbulent velocity, respectively. The parameter α hides the uncertainties associated with the source of the viscosity and is often estimated to be of the order of 0.01 (Hartmann et al. 1998; Andrews et al. 2010; Hughes et al. 2011).

Several mechanisms have been proposed as potential sources of viscosity responsible for the angular momentum transport in circumstellar disks including: thermal convection (Lin & Papaloizou, 1980; Ruden & Lin, 1986); shear instability (Dubrulle 1993); gravitational instability (Tomley et al. 1991; Laughlin & Bodenheimer 1994); and the so-called magneto-rotational instability (MRI, Balbus & Hawley 1991, 1998, 2000). Nevertheless, thermal convection and shear instability are not supported by hydrodynamical simulations to be effective mechanisms for angular momentum transport in disks (e.g., Balbus et al. 1996; Hawley et al. 1999; Stone et al. 2000). Gravitational instability could be important in early disk evolution stages but is unlikely to be a viable mechanism later on given the masses and surface densities of most CTTS disks. MRI is thus currently considered the most likely source of disk viscosity. However, it is believed that the gas in CTTSs is usually too cold and too weakly ionized for the MRI to be efficient beyond the upper layers of the disk. Typical CTTS disks are too dusty for the stellar X-rays to penetrate deep enough into the disk to ionize material to the level required by the MRI, resulting in a non-accreting "dead zone" in the disk midplane (Gammie 1996; Hartmann et al. 2006). It has been argued that the MRI can efficiently operate in special situations such as in the inner rims of transition disks with large inner opacity holes (Chiang & Murray 2007), but it can not explain the accretion rates observed in most CTTSs. The combination of MRI in the magnetically active surface layer of the disk and of gravitational instability in the deeper "dead" zones has been proposed as a possible solution (Hartmann et al. 2006). Nevertheless, the fundamental question, "what drives accretion in T Tauri disks?" has not yet been conclusively answered.

Viscous evolution models (Hartmann et al. 1998; Hueso & Guillot 2005) are broadly consistent with the observational constraints for disk masses and sizes discussed in §4. They can also reproduce the overall decline of accretion rates with stellar age that is observed (although with a very large scatter at any given age). However, pure viscous evolution models also predict a smooth, power-law evolution of the disk properties. This smooth disk evolution is inconsistent with the very rapid disk dissipation that usually occurs after a much longer disk lifetime (i.e. the "two-time-scale" problem). Viscous evolution models also fail to explain the variety of SEDs observed in the transition objects discussed in §7. These important limitations of the viscous evolution models show that they are in fact just a first-order approximation of a much more complex evolution involving several other important physical processes.

6.2 Photoevaporation by radiation from the central star

Together with viscous accretion, photoevaporation is one of the main mechanisms through which primordial circumstellar disks are believed to lose mass and eventually dissipate. Photoevaporation can be driven by energetic photons in the FUV ($6\,\mathrm{eV} < h\nu < 13.6\,\mathrm{eV}$), EUV ($13.6\,\mathrm{eV} < h\nu < 0.1\,\mathrm{keV}$) and X-ray

($h\nu > 0.1\,\mathrm{keV}$) energy range. Photons in each energy range affect the disks in different ways, and the relative importance of FUV, EUV, and X-ray photoevaporation is still not well understood. Photoevaporating photons can originate both at the central star and in neighboring massive stars. The latter scenario was discussed in §5.6.2 and here we focus on the former case.

6.2.1 Extreme UV photoevaporation Early photoevaporation models focused on the effect of ionizing EUV radiation (Hollenbach et al. 1994; Yorke & Welz, 1996; Richling & Yorke, 1997) on circumstellar gas around early-type stars. Later disk evolution models, known as "UV-switch" models, combine viscous evolution with photoevaporation by EUV photons (Clarke et al. 2001; Alexander et al. 2006a,b) to tackle the "two-time-scale" problem of T Tauri evolution (i.e., the sudden dispersion of the entire disk after much longer disk lifetimes, see §5.3). According to these models, extreme ultraviolet (EUV) photons originating at the stellar chromospheres of low-mass stars ionize and heat the circumstellar hydrogen to $\sim 10^4\,\mathrm{K}$. Beyond some critical radius, the thermal velocity of the ionized hydrogen exceeds its escape velocity and the material is lost in the form of a wind.

At early stages in the evolution of the disk, the accretion rate dominates over the evaporation rate and the disk undergoes standard viscous evolution: material from the inner disk is accreted onto the star, while the outer disk behaves as a reservoir that resupplies the inner disk, spreading as angular momentum is transported outwards. Later on, as the accretion rate drops to the photoevaporation rate, $\sim 10^{-10} - 10^{-9}\,M_\odot\,\mathrm{yr}^{-1}$ in the models, the outer disk is no longer able to resupply the inner disk with material. At this point, the inner disk drains on a viscous timescale ($\lesssim 10^5\,\mathrm{yr}$) and an inner hole of a few AU in radius is formed in the disk. Once this inner hole has formed, the inner disk edge is directly exposed to the EUV radiation and the disk rapidly photoevaporates from the inside out. Thus, the UV-switch model naturally accounts for the lifetimes and dissipation timescales of disks as well as for SEDs of some pre-main sequence stars suggesting the presence of large inner holes.

Recent high-resolution ($R \sim 30,000$) observations of the $12.81\,\mu$m [Ne II] line have provided the first observational evidence for ongoing EUV-driven photoevaporation on circumstellar disks. Pascucci et al. (2010) find that the [Ne II] line profiles and intensities from objects with inner opacity holes (i.e., transition disks) are in very good agreement with the predictions of the photoevaporation models by Alexander (2008). They also find that objects with optically thick inner disks do not show the same evidence for photoevaporating flows. This finding supports the idea that the formation of the inner hole exacerbates EUV-induced photoevaporation due to the direct irradiation of the inner rim.

6.2.2 EUV plus X-ray photoevaporation Recent models that include X-ray irradiation in addition to the EUV photon (Owen et al. 2010) show a similar qualitative behavior to photoevaporation by EUV alone, but also several important differences. Since X-rays are able to penetrate much lager columns of neutral gas than EUV photons, they are able to heat gas that is located deeper in the disk and/or at larger radii. While mass lost due to EUV photons is restricted to the inner few AU of the disk, X-rays can operate at tens of AU from the star. As a result, these models predict photoevaporation rates of the order of $10^{-8}\,M_\odot\mathrm{yr}^{-1}$, at least for the rather high X-ray luminosities assumed ($2\times10^{30}\,\mathrm{erg\,s}^{-1}$). These photoevaporation rate are up to two orders of magnitude

higher than those predicted by pure EUV photoevaporation models.

An important consequence of these higher photoevaporation rates are the relatively high disk masses ($\gtrsim 10\,M_{\rm Jup}$) expected at the time the inner hole is formed, which is expected to happen relatively early in the evolution of the disk. Since their models also predict that material should not flow inside the inner hole once the inner disk drains, one would expect to find a population of non-accreting pre-main sequence stars (e.g., WTTSs) with relatively massive disks. However, observations have shown (Andrew & Williams, 2005, 2007; Cieza et al. 2008, 2010) that WTTSs disks tend to have much lower masses ($< 1 - 2\,M_{\rm Jup}$). This suggests that, in reality, the photoevaporation rates and disk masses are lower than those predicted by Owen et al. (2010) when the inner hole is initially formed.

6.2.3 Far-UV plus X-ray photoevaporation Gorti et al. (2009) and Gorti & Hollenbach (2009) have recently modeled the photoevaporation of circumstellar disks by FUV, EUV and X-ray radiation. In their models, they assume very large initial disk masses ($\sim 100\,M_{\rm Jup}$) which produce high accretion rates. However, they obtained EUV photoevaporation rates that are much lower than those found by Alexander et al. (2006a,b). If only EUV photons were to be considered, therefore, it would tens of Myr, much longer than the observed lifetimes of primordial disks, to open up an inner hole. The outer disk would then survive for several Myr, which is inconsistent with the rapid transition from CTTS to diskless WTTS. They therefore discount EUV photoevaporation as an important mechanism.

Rather, in their models, the photoevaporation process is mostly driven by FUV photons operating on the outer disk ($R > 100\,{\rm AU}$), where loosely bound gas is heated and escapes as a neutral wind. For solar-type and lower mass stars, the FUV is mostly generated at the accretion shock, and its luminosity is therefore a function of the accretion rate until it plateaus at the value given by the FUV luminosity of the stellar chromosphere. They find that, even though X-ray photons do not produce significant photoevaporation by themselves, they indirectly increase the outflow rate by increasing the degree of ionization of the gas in the disk. This results in a higher electron population which in turns reduces the positive charge of the dust grains and thereby helps the FUV-induced grain photoelectric heating of the gas.

Just as the EUV+X-ray photoevaporation models of Owen et al. (2010), the FUV+X-ray models of Gorti et al. (2009) and Gorti & Hollenbach (2009) seem to over predict the mass and photoevaporation rates at the formation of the gap. They both predict a significant population of pre-main sequence stars with relatively massive ($\gtrsim 10\,M_{\rm Jup}$), non-accreting (or only mildly so) disks with large inner holes. The fact that such objects are extremely rare (see §7). suggests that the *quantitative* predictions of these models should be taken with caution.

6.3 Grain growth and dust settling

Even though solid particles only represent 1% of the initial mass of the disk, understanding their evolution is of utmost interest for disk evolution and planet formation studies. Solids not only dominate the opacity of the disk, but also provide the raw material from which the terrestrial planets and the cores of the giant planets (in the core accretion model) are made. While viscous accretion and the photoevaporation processes discussed above drive the evolution of the gas, other processes operate on the solid particles, most importantly, grain growth

and dust settling.

Grain growth and dust settling are intimately interconnected processes. Grains close to the surface of a disk would like to follow inclined Keplerian orbits, taking them in and out of the disk midplane. These motions are different from those of the gas, which is supported against gravity by its own pressure. Grains therefore experience a strong drag force from the gas. Small primordial dust grains ($r \sim 0.1\,\mu$m) have a very large surface to mass ratio and follow the gas motion. However, as primordial grains collide with each other, they eventually stick together by van der Waals forces and form large grains and aggregates of grains. As grains become larger, their surface to mass ratio decreases, their motions start to decouple from that of the gas, and start to settle toward the midplane. This increases the density of dust in the interior of the disk, which accelerates grain growth, and results on even larger grains settling deeper into the disk. If this process were to continue unimpeded, the end result would be a perfectly stratified disk with only small grains in the disk surface and large bodies in the midplane. However, since circumstellar disks are known to be turbulent, some degree of vertical stirring and mixing of grains is expected (Dullemond & Dominik 2005).

Observational support for grain growth in primordial disks is strong and comes from at least two independent lines of evidence: the shapes of the silicate features around 10 and 20 μm and the spectral slopes of disks at (sub-)millimeter wavelengths. These two lines of evidence provide information on two different populations of grains in the disk. The mid-infrared silicate emission features originate on the warm surface layer of the inner disk and probe grains in the submicron to a few micron size range. The (sub-)millimeter fluxes are dominated by the emission of the cold midplane of the outer disk, and probe larger bodies up to a few centimeters in size.

We first discuss the models and then the observational support for grain growth and settling.

6.3.1 Models Grain growth represents the baby steps towards planet formation. However, over 13 orders of magnitude in linear size separate sub-micron particles from terrestrial planets and many poorly understood processes operate along the way. Idealized dust coagulation models (i.e., ignoring fragmentation and radial drift) predict extremely efficient grain growth. Dullemond & Dominik (2005) investigated the dust coagulation process in circumstellar disks coupled to the settling and turbulent mixing of grains. They included 3 relatively well understood dust coagulation mechanisms (Brownian motion, differential settling and turbulence) and conclude that these processes are efficient enough to remove all small grains ($r < 100\,\mu$m) within 10^4 yr. This is clearly inconsistent with the wealth of observational evidence showing the presence of micron sized grains throughout the duration of the primordial disk phase discussed in the next section. These results strongly suggest that small grains must be replenished and that the persistence of small grains depends on a complex balance between dust coagulation and fragmentation (Dominik & Dullemond 2008).

Recent, more realistic models including fragmentation and radial drift confirm the necessity of grain fragmentation to explain the ubiquity of small grains in disks (Brauer et al. 2008; Birnstiel et al. 2010). These same models also confirm the severity of the problem known as the "meter-size barrier", a physical scale at which solids are expected to suffer both destructive collisions and removal through rapid inward migration (Weidenschilling 1977). Even though several possible

solutions have been proposed, including the formation of planetesimals in long-lived vortices (e.g., Heng & Kenyon, 2010) or via the gravitational instability of millimeter-sized chondrules in a gas deficient subdisk (e.g., Youdin & Shu, 2002), overcoming the "meter-size barrier" still remains one of the biggest challenges for planet formation theories (Chiang & Youdin 2009).

6.3.2 Evidence for grain growth from sub-micron to microns Pristine dust in the interstellar medium is composed primarily of amorphous silicates, generally olivine and pyroxene with characteristic features at 9.7 and 18.5 μm from Si–O stretching and O–Si–O bending modes, respectively. The shape of these features is a sensitive diagnostic of the size of small grains, in the $r \sim 0.1-5\,\mu$m range. While the emission features of the smallest grains are strong and narrow, those of larger particles are weaker and broader. Thermal annealing can modify the lattice structure of olivine and pyroxene and turn them into their crystallized forms, known as enstatite and forsterite. These crystalline silicates have multi-peak features at slightly longer wavelengths than their amorphous counterparts.

Recent surveys with the IRS on *Spitzer* have allowed the study of silicates in hundreds of circumstellar disks in nearby star-forming regions (Kesser-Silacci et al. 2006; Furlan et al. 2006,2009; Oliveria et al. 2010; McClure et al. 2010). Since these observations probe the warm optically thin disk "atmosphere" and the larger particles are expected to settle toward the disk interior, they provide information on the smallest population of grains present in the disk. Nevertheless, the observed silicate features in most disks are consistent with the presence of micron-sized particles and the absence of sub-micron dust grains. This implies either that grain growth is more efficient than fragmentation at these scales or that sub-micron grains are efficiently removed from the upper layers of the disk by stellar winds or radiation pressure (Olofsson et al. 2009).

These *Spitzer* surveys have also shown that the signatures of grain growth and crystallization are seen at very early stages of disk evolution, even before the envelope has dissipated (Furlan et al. 2009; McClure et al. 2010). Also, there seems to be little connection between the age or evolutionary stage of a primordial disk and the dust properties probed by the silicate features. Even though many studies have searched for a correlation between the large scale properties of the disk (e.g., mass, accretion rates) and grain characteristics (sizes, degree of crystallization), no conclusive evidence has yet been found (e.g., Kesser-Silacci et al. 2006; Furlan et al. 2009; Oliveria et al. 2010). This lack of correlation between age and dust properties suggest that the characteristics of the dust population depend on a balance between grain growth and destruction and between crystallization (via thermal annealing) and amorphization (e.g., via X-ray irradiation, Glauser et al. 2009). This balance seems to persist throughout the duration of the primordial disk stage, at least in the surface layers of the disk.

The fraction of circumstellar disks showing crystalline features and the relative incidence of the different features ($\lambda \sim 10\,\mu$m versus $\lambda > 20\,\mu$m) vary greatly from study to study. While Watson et al. (2009) find that 90% of T Tauri disks in their sample show either the 9.2 μm estatite or the 11.3 μm forsterite features, these features are only identified in 20% of T Tauri stars observed by Olofsson et al. (2009). Also, while the former study concludes that crystallization is higher than at the regions probed by the 10 μm silicate feature ($r \sim 1\,$AU), the latter argues that crystallization is more common in the regions probed by the

$20-30\,\mu$m features ($r \sim 10\,$AU). The discrepancies are likely to be related to the different techniques used by different teams to identify crystalline silicates and the difficulties of distinguishing crystallization from grain growth. However, ground-based mid-infrared interferometric observations have shown a clear crystallinity gradient in the inner disks of at least 3 Herbig AeBe stars (van Boekel et al. 2004). The highest crystallinity is seen in the hot inner disk ($r \sim 1-2\,$AU). This is expected because the formation of crystalline silicates through thermal annealing requires temperatures of the order of 1000 K. Indeed, the very fact that some crystalline features are also seen at $20-30\,\mu$m, a wavelength range that probes much cooler material farther out in the disk, points towards a significant degree of radial mixing of dust particles (Olofsson et al. 2009).

6.3.3 Evidence for grain growth from microns to millimeters A second, independent line of evidence for grain growth is found in the slope, $\alpha_{\rm mm}$, of the SED at submillimeter wavelengths, $F_\nu \propto \nu^{\alpha_{\rm mm}}$. The slope between $\lambda \approx 0.5-1\,$mm is significantly shallower in protoplanetary disks, $\alpha_{\rm mm} \approx 2-3$ (Beckwith & Sargent 1991; Mannings & Emerson 1994; Andrews & Williams 2005, 2007) than in the diffuse interstellar medium, $\alpha_{\rm mm} \sim 4$ (Boulanger et al. 1996). In the Rayleigh-Jeans limit, the flux, $F_\nu \propto B_\nu(1-e^{-\tau_\nu}) \rightarrow \nu^2$ for optically thick emission and $\rightarrow \kappa_\nu \nu^2$ for optically thin emission. The SED slope is therefore bound between $\alpha_{\rm mm} = 2$ and $2+\beta$ (see equation 2). Unresolved photometric observations include some optically thick emission from the inner disk so the connection between the observed disk average $\alpha_{\rm mm}$ and the grain opacity index, β, requires modeling the surface density profile (Beckwith et al. 1990). For a simple power law thin disk model, Andrews & Williams (2005) show that $\alpha_{\rm mm}-\beta$ lies between 1.1 and 1.8 for disk masses $10^{-2}-10^{-5}\,M_\odot$ respectively, and is approximately independent of $\alpha_{\rm mm}$. Beckwith & Sargent (1991) and Mannings & Emerson (1994) make similar corrections and all reach the same conclusion that the grain opacity index is significantly lower in disks, $\beta_{\rm disk} \approx 0.5-1$, than in the interstellar medium, $\beta_{\rm ISM} \approx 1.7$.

The decrease in the dust opacity index is best explained by the presence of substantially larger dust grains in disks relative to the interstellar medium. For a power law distribution of grain sizes, $n(a) \propto a^{-p}$, D'Alessio et al. (2001) and Natta et al. (2004) show that $\beta \approx 1.7$ if the maximum grain size $a_{\rm max} < 30\mu$m but then decreases to $\beta \lesssim 1$ for $a_{\rm max} \gtrsim 0.5\,$mm. Draine (2006) provides a useful relation, $\beta \approx (p-3)\beta_{\rm ISM}$ if $a_{\rm max}$ is more than 3 times the observing wavelength, largely independent of grain composition. The implication of shallow disk SED slopes at submillimeter wavelengths relative to the interstellar medium is that dust grains have grown by at least 3 orders of magnitude, from microns to millimeters.

Some grain growth appears to happen in dense molecular cores before disks form. Shirley et al. (2000) measures the spectral slope for 21 cores, some pre-stellar, others in very early stages of low mass star formation and find an average spectral slope between 450 and $850\,\mu$m of $\alpha_{\rm mm} = 2.8$, which is intermediate between the diffuse interstellar medium and protoplanetary disks. Kwon et al. (2009) model multi-wavelength $1.3-2.7\,$mm observations of Class 0 cores and derive an opacity index, $\beta \approx 1$, which is also shallower than the diffuse interstellar medium but not quite as steep as in protoplanetary disks.

There is also evidence that grain growth continues throughout the disk lifetime. Andrews & Williams (2005) find a significant difference in the SED slope between

Taurus Class I (median $\alpha_{\rm mm} = 2.5$) and Class II disks (median $\alpha_{\rm mm} = 1.8$). They also show that the submillimeter and infrared SED slopes are correlated with a best fit linear relationship, $\alpha_{\rm mm} = 2.09 - 0.40\alpha_{\rm IR}$.

These sub-millimeter data only place a lower bound on the size of the most massive grains. Longer wavelength observations constrain the presence of larger grains but the flux decreases (as the surface area of the dust decreases for a given mass) and the free-free emission from an ionized stellar wind often dominates for $\lambda \gtrsim 1\,$cm (Natta et al. 2004). On the other hand, the correction for an opaque inner region is smaller. Surveys of Taurus disks have been carried out at 7 mm by Rodmann et al. (2006) and at 3 mm by Ricci et al. (2010a) who both find that the shallow SED slope generally extends to their observing wavelength and infer average opacity indices, $\langle\beta\rangle = 1, 0.6$ respectively. Ricci et al. (2010b, 2011) find similar results for Ophiuchus and Orion disks. The implication is that centimeter sized particles are commonplace. The longest wavelength detection of dust in a protoplanetary disk to date was carried out by Wilner et al. (2005). By resolving the nearby, bright TW Hydra disk and showing that its flux is constant with time, they convincingly show that the 3.5 cm emission is from thermal dust emission and not accretion shocks or a stellar wind. The Draine (2006) formulation would therefore indicate the presence of $\sim 10\,$cm sized "pebbles" (or snowballs) in the disk out at least to the 15 AU beam.

Resolved images showing the surface density profile and size of the disk allow more precise opacity corrections to be made (Testi et al. 2001, 2003; Rodmann et al. 2006). Collisional grain growth (Blum & Wurm 2008) is expected to have a strong radial dependence due to the decreasing density and Keplerian velocity with increasing radius. Isella et al. 2010 resolve the RY Tau and DG Tau disks at $\lambda = 1.3$ and 2.8 mm and model the data with a radially dependent dust opacity. However, to within their precision, $\Delta\beta = 0.7$, they do not see a significant gradient.

6.3.4 Evidence for dust settling Circumstellar disks are flared (see §4.3.2) and hence intercept and reprocess more stellar radiation than physically thin, optically thick disks. Nevertheless, most T tauri stars exhibit less mid-infrared emission than expected for a disk in hydrostatic equilibrium. This can be understood in terms of dust settling with which reduces the scale height and flaring angle of the disk (Dullemond & Dominik 2004). Mid-infrared slopes can therefore be used as a diagnostic of dust settling. D′Alessio et al. (2006) explored parametric models with two populations of grains: micron sized grains with a reduced dust-to-gas mass ratio in the surface layers of the disk, and mm-sized grains with an increased dust-to-gas mass ratio in the disk midplane. In order to quantify the degree of dust settling, they introduced the parameter ϵ, the ratio of the dust-to-gas mass ratio in the surface layer of the disk to the standard dust-to-gas mass ratio of the interstellar medium (1:100). In this context, $\epsilon = 1$ implies that no dust settling has occurred, and ϵ decreases as dust settling increases. D′Alessio et al. (2006) find that the median mid-infrared slopes of CTTSs can be reproduced with models where $\epsilon \leq 0.1$.

Furlan et al. (2006) applied these parametric models to reproduce the spectral slopes of a large sample (> 80) of Taurus T Tauri stars observed with the *Spitzer* Infrared Spectrograph. They conclude that most objects are consistent with dust depletion factors in the surface layers of the disk of order of 100 to 1000 (i.e., corresponding to $\epsilon = 0.01$ to 0.001). A similar result is found by McClure et al.

(2010) in the Ophiuchus molecular cloud. They also find evidence for significant dust settling in young (age $\sim$ 0.3 Myr) objects embedded in the cloud core, suggesting that this process sets in early in the evolution of the disk (see also Furlan et al. 2009).

6.4 Typical devolution and diversity of evolutionary paths

Although we are far from fully understanding the complex evolution of primordial circumstellar disks, a coherent picture is starting to emerge from the many models and observational constraints discussed above. While it is clear that not all disks follow the same evolutionary path, many observational trends suggest that most objects do follow a common sequence of events. In what follows we summarize our current understanding of the "typical" evolution of a circumstellar disk.

6.4.1 The evolution of a typical disk Early in its evolution, the disk loses mass through accretion onto the star and FUV photoevaporation of the outer disk (Gorti et al. 2009). The FUV photoevaporation is likely to truncate the outer edge of the disk, limiting its viscous expansion to a finite size of several hundreds of AU in diameter (Figure 7a). During this "mass depletion" stage, which can last several Myr, an object would be classified as a Classical T Tauri star based on the presence of accretion indicators. Accretion is likely to be highly variable in short timescales, but show a declining long-term trend.

At the same time, grains grow into larger bodies that settle onto the mid-plane of the disk where they can grow into rocks, planetesimals and beyond. Accordingly, the scale height of the dust decreases and the initially-flared dusty disk becomes flatter (Figure 7b). This steepens the slope of the mid and far-infrared SED as a smaller fraction of the stellar radiation is intercepted by circumstellar dust (Dullemond & Dominik 2005). The near-infrared fluxes remain mostly unchanged because the inner disk stays optically thick and extending inwards to the dust sublimation temperature. The most noticeable SED change during this stage is seen in the decline of the (sub-)millimeter flux, which traces the decrease in the mass of millimeter and smaller sized particles (Andrews & Williams, 2005, 2007; Lee et al. 2011; Figure 8.

As disk mass and accretion rate decrease, EUV photons from the stellar chromosphere are able to penetrate the inner disk and EUV-induced photoevaporation becomes important. When the accretion rate drops to the EUV photoevaporation rate ($\sim 10^{-10} - 10^{-9}\,M_\odot\,\mathrm{yr}^{-1}$), the outer disk is no longer able to resupply the inner disk with material (Alexander et al. 2006). At this point, the inner disk drains on a viscous timescale ($\lesssim 10^5\,\mathrm{yr}$) and an inner hole of a few AU in radius is formed in the disk (Figure 7c). Once this inner hole has formed, the EUV photons can reach the inner edge of the disk unimpeded, and the EUV-photoevaporation rate increases further, preventing any material from the outer disk from flowing into the inner hole. This halts accretion and results in the rapid transition between the classical T Tauri star to the weak-line T Tauri star stage.

The formation of the inner hole marks the end of the slow "mass depletion" phase and the beginning of the of the rapid "disk dissipation" stage. By the time the inner hole is formed, the mass of the outer disk is believed to be $\lesssim 1-2\,M_{\mathrm{Jup}}$, as attested by the low mass of WTTS disks (Andrews & Williams 2005, 2007; Cieza et al. 2008, 2010). During this "disk dissipation" stage, the SEDs of the WTTS disks present a wide range of morphologies, as expected for disks with inner holes of different sizes (Padgett et al. 2006, Cieza et al. 2007, Wahhaj,

2010). Once the remaining gas photoevaporates, the dynamics of the solid particles become driven by radiation effects (Figure 7d). While the small ($r \lesssim 1\,\mu$m) grains are quickly blown out by radiation pressure, slightly larger ones spiral in due to the Poynting-Robertson effect and eventually evaporate when they reach the dust sublimation radius. What is left represents the initial conditions of a debris disk: a gas poor disk with large grains, planetesimals and/or planets. The fact that the vast majority of WTTSs show no evidence for a disk (primordial or debris) implies that not *every* primordial disk will evolve into a *detectable* debris disks. Whether *some* disks remain detectable throughout the primordial to debris disk transition or there is always a quiescent period between these two stages still remains to be established.

6.4.2 The age variable While it is true that there is some discernible correlation between the ages of pre-main sequence stars and the evolutionary stages of their disks, this correlation is rather weak. In fact, circumstellar disks in every stage of evolution, from massive primordial disks to debris disks and completely dissipated disks, are seen in stellar clusters and associations with ages ranging from $\lesssim 1$ Myr to ~ 10 Myr (e.g., Muzerolle et al. 2010). Diskless WTTSs in the core of the young Ophiuchus molecular cloud and the relatively old, gas-rich TW Hydra are good examples of these extremes. This weak correlation between stellar age and disk evolutionary stage can be explained by the combination of two factors: the wide range in the duration of the "mass depletion" stage and the short time scale of the "disk dissipation" phase. On the one hand, as discussed in §5.6.1, circumstellar disks in medium separation binary systems are likely to have truncated disks with small initial masses. Since the "mass depletion" stage in such objects is expected to be very short ($\lesssim 0.3$ Myr), their circumstellar disks can easily go through all the evolutionary stages described above in less than 1 Myr. On the other hand, initially massive circumstellar disks evolving in isolation can in principle remain optically thick at all infrared wavelengths for up to ~ 10 Myr.

6.4.3 Evidence for alternative evolutionary paths The observed properties of most circumstellar disks are consistent with the evolutionary sequence shown in Figure 10; however, many outliers do exist, showing that not all disks follow the same sequence of event in an orderly manner. Perhaps the most intriguing outliers are accreting objects that have cleared-out inner disks but retained massive ($> 10\,M_{\rm Jup}$) outer disks. Examples of such objects, which represent a small subgroup of the so-called transition disks, include DM Tau, GM Aur (Najita et al. 2007), and RX J1633.9-2442 (Cieza et al. 2010). Since the presence of accretion and their large disk masses make their inner holes incompatible with the predictions of photoevaporation models, these objects do not fit into the evolutionary sequence discussed above, and it is reasonable to assume that additional processes are in play. The nature of these objects is discussed in some detail in the following section, on transition circumstellar disks.

6.5 Section summary

- Circumstellar disks evolve through a variety of processes, including viscous accretion and spreading, photoevaporation by FUV, EUV, and X-ray radiation, grain growth and dust settling, and dynamical interaction with (sub)stellar and planetary-mass companions.

- Even though viscous accretion is arguably the most fundamental disk evolution process, the source of viscosity responsible for the angular momentum transport still remains to be established.
- Together with viscous accretion, photoevaporation is one the main mechanisms through which primordial circumstellar disks are believed to lose mass and eventually dissipate. Photons in each energy range operate in different ways, and the relative importance of FUV, EUV, and X-ray photoevaporation is still not well understood.
- While viscous accretion and the photoevaporation processes drive the evolution of the gas, two intimately connected processes, dust settling and grain growth, operate on the solid particles. These latter processes are believed to represent the initial steps towards the formation of terrestrial planets (and also of giant planets in the core accretion model). There is strong evidence for solid particles growing to the mm (and even cm) scale in circumstellar disks, but the presence and size distribution of larger bodies remain unconstrained.
- Both dust settling and grain growth have strong effects on the observed SEDs. Dust settling steepens the mid- and far-infrared slopes. Grains growth has the opposite effect on the (sub)mm slopes and can also reduce near-infrared emission from the inner disk.
- Most circumstellar disks are likely to go through a slow "mass depletion" phase followed by a rapid "disk dissipation" stage: they first lose mass through viscous accretion and FUV photoevaporation and then dissipate from the inside out through EUV photoevaporation. A wide range in the duration of the "mass depletion" stage and the short time scale of the "disk dissipation" phase weaken any expected correlation between stellar age and disk evolutionary stage.
- On top of the disk evolution processes described above, a small fraction ($\sim 10\%$) of disks develop sharp inner holes due to dynamical interactions with (sub)stellar and planetary-mass companions. These holes result in the characteristic SED dip seen in some transition disks.

7 TRANSITION DISKS

Transition disks were first identified by *IRAS* as objects with little or no excess emission at $\lambda < 10\,\mu$m and a significant excess at $\lambda \geq 10\,\mu$m (Strom et al. 1989; Wolk & Walter 1996). The lack of near-infrared excess was interpreted as a diagnostic of inner disk clearing possibly connected to the early stages of planet formation. Because of this possible connection, transition disks have received special attention in circumstellar disks studies even though they represent a small percentage ($\lesssim$ 10-20%) of the disk population in nearby star-forming regions. In this section we discuss the diversity of SED morphologies presented by transition disks, their incidence and range of physical properties, and their connection to planet formation and other disk evolution processes.

7.1 The diversity of transition disk SEDs

Transition disks present a variety of infrared SED morphologies and their diversity is not properly captured by the traditional classification scheme of young stellar

objects (i.e., the Class I through III system, see § 2). In order to better describe the shape of transition disk SEDs, Cieza et al. (2007) introduced a two-parameter scheme based on the longest wavelength at which the observed flux is dominated by the stellar photosphere, $\lambda_{\rm turn-off}$, and the slope of the infrared excess, $\alpha_{\rm excess}$, computed from $\lambda_{\rm turn-off}$ to 24 μm.

Because of their diversity, the precise definition of what constitutes a transition object found in the disk-evolution literature is far from homogeneous. Transition disks have been defined as objects with no detectable near-infrared excess, steep slopes in the mid-infrared, and large far-infrared excesses (Muzerolle et al. 2010; Sicilia-Aguilar et al. 2010). This definition is the most restrictive one and effectively corresponds to objects with $\lambda_{\rm turn-off} \gtrsim 4.5 - 8.0\,\mu$m and $\alpha_{\rm excess} > 0$. The above definition has been relaxed by some authors (Brown et al. 2007; Merin et al. 2010) to include objects with small, but still detectable, near-infrared excesses. Transition disks have also been more broadly defined in terms of a significant decrement relative to the median SED of CTTSs at any or all infrared wavelengths (Najita et al. 2007, Cieza et al. 2010). Several names have recently emerged in the literature to identified subclasses of transition disks. Objects with no detectable near-infrared excess and $\alpha_{\rm excess} > 0$ have been called "classical" transition disks (Muzerolle et al. 2010), while other objects with a sharp rise in their mid-infrared SEDs have been termed "cold disks" (Brown et al. 2007, Merin et al. 2010) regardless of the presence of near-infrared excess. Disks with a significant flux decrement at all infrared wavelengths relative to the SED of an optically thick disk extending the dust sublimation temperature have been referred to as "anemic" disks (Lada et al. 2006), "homologously depleted" disks (Currie et al. 2009), or "weak excess" disks (Muzerolle et al. 2010). Finally, disks with evidence for an optically thin (in the infrared) gap separating optically thick inner and outer disk components have been called "pre-transition" disks (Espaillat et al. 2007, 2010) since they are believed to be precursors of objects with sharp, but empty inner holes (i.e., the "classical" transition disks mentioned above). Examples of the different types of transition disks are shown in Figure 11.

7.2 Interpretation of transition disk SEDs

Understanding the physical processes responsible for the diversity of transition disks and its implications for planet formation is currently one of main challenges in the field. There seem to be two *physically* distinct families of transition disks: objects with falling ($\alpha_{\rm excess} \lesssim 0$) and rising ($\alpha_{\rm excess} > 0$) mid-infrared SEDs. The former group has in general been interpreted as evidence for grain growth and dust settling toward the midplane (Lada et al. 2006; Sicilia-Aguilar et al. 2010; Cieza et al. 2010). Both processes tend to reduce the mid-infrared fluxes. Grain growth removes small grains and thus reduces the opacity of the inner disk. Dust settling results in flatter disks that intercepts and reprocess and smaller fraction of the stellar radiation. This group of objects includes anemic, homologously depleted disks, and weak-excess disks.

Objects with rising mid-infrared SEDs, a group that includes classical transition disks, cold disks, and pre-transition disks, are more consistent with a strong radial dependence in the dust opacity resulting in a sharp inner opacity hole. Several configurations exist however. The hole can be mostly empty of *dust*, resulting in a complete lack of near infrared excess as in the case of DM Tau

(Calvet et al. 2005) and Coku Tau 4 (D'Alessio et al. 2005), or presumably filled by optically thin dust such as TW Hydra (Calvet et al. 2002) or GM Aur (Hughes et al. 2009). Alternatively, an optically thick inner annulus can exist within the much larger inner hole, which seem to be the case for the pre-transition disks LkCa 15 and UX Tau A, whose near-infrared excesses are well reproduced by an inner wall at the dust sublimation temperature (Espaillat et al. 2010).

7.3 Physical processes behind transition disk SEDs

The inner opacity holes of some transition disks have been suspected to be signposts of planet formation since they were first identified by *IRAS*, years before the first extrasolar planets were identified. Strom et al. (1989) suggested they could be an indication of circumstellar dust assembling into larger bodies, a process that corresponds to the first stages of planet building. Strictly speaking, inner opacity holes only indicates a lack or deficiency of small ($\lesssim 1\,\mu$m) dust grains in the inner disk. As discussed in §6.3, once primordial sub-micron dust grains grow into somewhat larger bodies ($\gg 1\,\mu$m), most of the solid mass ceases to interact with the stellar radiation, and the opacity function decreases dramatically. The effects on the SED of grains growing into terrestrial planets are no different from those of growing into meter size objects. In other words, an SED contain very little information on how far along terrestrial planet formation has processed in a given disk.

The formation of a giant planet, on the other hand, is expected to have a dramatic effect on the SED. Theoretical models of the dynamical interactions of forming giant planets with the disk (Lin & Papaloizous 1979, Artymowicz & Lubow 1994) predict the formation of tidal gaps and inner holes that are consistent with the *sharp* inner holes inferred for transition disks with $\alpha_{\rm excess} \gtrsim 0$. However, several other disk evolution processes can in principle produce similarly sharp holes, including grain growth, photoevaporation, and dynamical interactions with (sub)stellar companions.

Grain growth could, at least in principle, be a strong function of radius and form a sharp inner opacity hole as it is expected to be more efficient in the inner regions where the surface density is higher and the dynamical timescales are shorter (Dullemond & Dominik 2005). The formation of an inner hole is also one of the stages predicted by photoevaporation models (see §6.2). Finally, circumbinary disks are expected to be tidally truncated and have inner holes with a radius about twice the orbital separation (Artymowicz & Lubow 1994). Distinguishing between (giant) planet formation and the processes mentioned above thus require additional observational constraints. For instance, stellar companions can be identified with a combination of adaptive optics imaging and radial velocity observations. Similarly, disk masses and accretion rate information can be used to identify inner holes carved by photoevaporation as in this case the disk is expected to have low mass ($M_{\rm disk} \lesssim 5\,M_{\rm Jup}$) and negligible accretion (Alexander et al. 2006). More recent photoevaporation models (Owen et al. 2010) predict higher photoevaporation rates and can accommodate larger disk masses at the time of the hole formation ($\sim 10 - 20\,M_{\rm Jup}$). However, as discussed in §6.2.3, these models predict a significant population of WTTSs with relatively massive disks which does not seem to be a consistent with the observations of WTTS disk masses (Andrews & Williams, 2005,2007; Cieza et al. 2008, 2010).

7.4 The incidence of transition disks

Establishing the incidence of transition disks is not straightforward given the very diverse definitions used by different studies. Also, samples are usually not complete and thus suffer from several selection effects. Furthermore, several background objects can mimic the SEDs of some types of transition disks and skew the statistics. In particular, Asymptotic Giant Branch stars and classical Be stars can be easily confused by with "weak excess" transition disks (Oliverira et al. 2010; Cieza et al. 2010) and the SEDs of edge-on disks can look like those of cold disks (Merín et al. 2010).

With these caveats, the fraction of disks in nearby star-forming regions that are seen in a transition stage is thought to be $\lesssim 10-20\%$ (Lada et al. 2006; Hernandez et al. 2007; Dahm & Carpenter 2009; Currie et al. 2009; Kim et al. 2009, Fang et al. 2009). Also, it is clear that "weak-excess" (or "anemic" and "homologously depleted") transition disks outnumber, by factors of ~ 2 to ~ 3, objects with sharp inner holes (Muzerolle et al. 2010; Cieza et al. 2010). Weak-excess disks seem to be more common in older clusters (Murzerolle et al. 2010). This is expected because disks should become flatter and lose mass with time (see §6.4). Weak-excess disks are also much more abundant around young (age $\sim 1\,$Myr) M-stars than around solar-type stars of the same age (Sicilia-Aguilar et al. 2008). However, this is very likely to be a luminosity effect rather than an evolutionary one. Since M-type stars are much fainter and cooler than solar-type stars, they may present weak mid-infrared excess emission even if the disk extends in to the dust sublimation radius (Ercolano et al. 2009).

The relatively small number of objects seen in a transition stage suggests that the evolutionary path through a transitional disk is either uncommon or rapid. However, observations show that an infrared excess at a given wavelength is always accompanied by a *larger* excess at longer wavelengths, out to $\sim 100\,\mu$m. This implies that, unless some disks manage to lose the near-, mid-, and far-infrared excess at *exactly* the same time, the near-infrared excess always dissipates before the mid-infrared and far-infrared excess do. No known process can remove the circumstellar dust at all radii simultaneously, and even if grain growth, a close binary, or planet formation do not produce an inner hole, EUV photoevaporation by the central star will do so once the accretion rate through the disk falls below the photoevaporation rate. Therefore, it is reasonable to conclude that transition disks represent a common but relatively short phase in the evolution of a circumstellar disk. Of course, how long the transition stage lasts for a given disk strongly depends on the nature of each object. On the one hand, the transition phase should be very short ($< 0.5\,$Myr) if the inner hole is formed through photoevaporation. On the other hand, an object could in principle show a transition disk SED for a longer period of time if the inner opacity hole is due to grain growth, or giant planet formation.

7.5 The physical properties of transition objects

While it is clear that many different processes can result in transition disk SEDs, the relative importance of these processes is still not well understood. Distinguishing among processes requires additional observational constraints on the physical properties of these objects, such as disk mass, accretion rates, fractional disk luminosities ($L_{\rm disk}/L_{\rm star}$), and multiplicity information. These observational

constraints have only recently been obtained for statistically significant samples of transition disks.

Najita et al. (2007) investigated the SEDs, disk masses, and accretion rates of over 60 Taurus pre-main sequence stars and identified 12 transition disks. Based on their SEDs, 7 of their objects could be further classified as weak excess disks (CX Tau, DN Tau, FO Tau, FQ Tau, GO Tau, V773 Tau and V836 Tau), 3 as classical transition disks (Coku Tau 4, DM Tau, and GM Aur), and 2 as pre-transition disks (LkCa 15 and UX Tau). They found that the transition disks in their sample have larger average disk masses and lower average accretion rates than non-transition disks around single stars. They concluded that, with the exception of Coku Tau 4, they were all more consistent with the giant planet formation scenario than with photoevaporation (which would require negligible accretion rates and lower disks masses) and grain growth (which would favor higher accretion rates for a given disk mass). However, since their sample was drawn from the *Spitzer* spectroscopic survey of Taurus presented by Furlan et al. (2006), who in turn selected their targets based on mid-infrared colors from *IRAS*, their sample was clearly biased towards the brightest objects in the mid-infrared and are unlikely to represent the overall population of transition disks. As a counter example, Cieza et al. (2008) studied over 20 WTTSs with transition disk SEDs, found that all had very small disk masses ($\lesssim 2\,M_{\rm Jup}$), and concluded they were all consistent with photoevaporation. Sicilia-Aguilar (2010) studied accretions rates in a sample of 95 members of the $\sim 4\,$Myr Tr 37 cluster. They found that half of the 20 *classical* transition disks in their sample had evidence for accretion (i.e. their holes contain gas but no dust) and half were non-accreting (i.e., their holes are really empty). Furthermore, the accretion rates they estimates for transition disks were indistinguishable from those of regular CTTSs in the cluster, a result that is at odds with the Taurus sample studied by Najita et al. (2007). These discrepancies show that transition disks are a highly heterogeneous group of objects and that the mean properties of a given sample are highly dependent on the details of the sample selection criteria and thus should be interpreted with caution.

Cieza et al. (2010) studied a sample of 26 transition disks in Ophiuchus. With the exception of edge-on disks, highly embedded objects, and the lowest mass transition objects, all of which are too faint in the optical to pass one of their selection criteria, the sample is likely to be representative of the entire transition disk population in the Ophiuchus molecular cloud. They find that nine of the 26 targets have low disk masses ($< 2.5\,M_{\rm Jup}$) and negligible accretion, and are thus consistent with photoevaporation. However, four of these nine non-accreting objects have fractional disk luminosities $< 10^{-3}$ and could already be in a debris disk stage. Seventeen of their transition disks are accreting. Thirteen of these accreting objects are consistent with dust settling and grain growth ($\alpha_{\rm excess} \lesssim 0$), while the remaining four accreting objects have SEDs suggesting the presence of sharp inner holes ($\alpha_{\rm excess} > 0$), and thus are candidates for harboring embedded giant planets (see Figure 11). Interestingly, non-accreting objects with relatively massive disks ($\gtrsim 3\,M_{\rm Jup}$) are absent in their sample. Such objects are rare but do exist. The "cold disk" around T Cha is an example (Brown et al. 2007), and its properties could be explained by a companion massive enough to halt accretion onto the star. Nevertheless, a few accreting binary systems are also known (e.g., DQ Tau, Carr et al. 2001 and CS Cha Espaillat et al. 2007), which implies that a massive companion does not always stops accretion. The eccentricity of

the orbit, and the viscosity and scale height of the disk also determine whether accretion onto the star cana continue (Artymowicz & Lubow 1996).

Binarity is also known to result in transition disk SEDs. However, identifying close companions is particularly difficult, especially if they are within the inner $\sim 5 - 10$ AU of the disk, which is beyond the near-infrared diffraction limit of $8 - 10$ m class telescopes at the distance of the nearest star-forming regions ($\sim 125-140$ pc). Using the aperture masking technique in a single Keck telescope, Ireland & Krauss (2008) showed that CoKu Tau 4 is near-equal mass binary system, which explains the sharp hole that had been inferred from its SED; nevertheless, it is clear that not all sharp inner holes are due to binarity. DM Tau, GM Aur, LkCa 15, UX Tau, and RY Tau have all been observed with the Keck interferometer (Pott et al. 2010). For these objects, all of which show evidence for accretion unlike CoKu Tau 4, stellar companions with flux ratios $\lesssim 20$ can be ruled out down to sub-AU separations.

7.6 Resolved observations of transition disks

While SED modeling provides strong evidence for the presence of inner holes in some transition disks, this evidence is indirect and model-dependent. Long baseline interferometry at (sub-)millimeter wavelengths, on the other hand, can directly image the inner holes of the most massive transition disks in nearby star-forming regions.

Inner holes have been resolved in a growing number of transition disks including LkCa 15, MWC 480 (Pietu et al. 2006), TW Hydra (Hughes et al. 2007), GM Auriga (Hughes et al. 2009), LkHα 330, SR 21N, and HD 135344B (Brown et al. 2009), WSB 60, DoAr 44 (Andrews et al. 2010), and J1604-2130 (Mathews et al. 2011). A montage of resolved submillimeter images of transition disks is shown in Figure 12.

Since the emission is optically thin in these (sub-)millimeter data, the images directly show the mass surface density profile of the disk and can be used to measure the size and sharpness of inner holes. In most cases, the (sub-)millimeter interferometry confirms the expected sizes of the inner holes (ranging from ~ 4 AU to ~ 50 AU in radius) and their sharpness (i.e., a large increase in the dust density over a small range in radii) predicted from the SED. For example, Brown et al. (2009) showed the inner holes in LkHα 330, SR 21N, and HD 135344B were consistent with step functions with a surface density reduction of ~ 1000 and radii of 47, 33, and 39 AU respectively.

The details in these images may contain dynamical hints of giant planets. These include azimuthal asymmetries, such as HD 135344B (Brown et al. 2009) and a warp between the dust and gas structures in GM Aur (Hughes et al. 2009). Still, since circumstellar disks are only barely resolved by current interferometers and the signal to noise of most images is modest at best, these are no more than suggestions at the moment. High fidelity images with *ALMA* will soon allow us to study the structure of circumstellar disks in much greater detail, and the incidence of radial gaps, density waves, and other possible azimuthal asymmetries should become evident. It may well also be possible to find earlier stages in the disk clearing process through a decline in the millimeter flux before the infrared opacity drops below one (Andrews et al. 2008).

In addition to the (sub-)millimeter images discussed above, in at least one case, LkCa 15, the inner hole has been imaged in the near-infrared from starlight

reflected from the edge of a disk wall $\sim 50\,\mathrm{AU}$ in radius (Thalmann et al. 2010), once again confirming the structure inferred from modeling the SED of the object.

7.7 Transition disks, disk evolution, and planet formation

As discussed in § 7.3, transition disk SEDs can result from several physical processes such as grain growth, photoevaporation, dynamical interactions with (sub)stellar companions, and giant planet formation. All these processes have distinct observational signature and can be distinguished with appropriate datasets. Transition disks hence represent prime targets to study because they can provide invaluable observational constraints for disk evolution and planet formation theory.

From extrapolation of the results from radial velocity surveys, it is currently believed that $\sim 20\%$ of main sequence solar-type stars in the solar neighborhood have giant planets ($M \sin i \gtrsim 0.3\,M_{\mathrm{Jup}}$) within 20 AU (Cumming et al. 2008). Statistically, therefore, we should have observed many primordial disks with young giant planets embedded in them. Accreting transition disks with sharp inner holes around single stars are the best candidates to be the sites of ongoing giant-planet formation. Their sharp holes could be explained by either photoevapotation or the dynamical interaction with an embedded object. However, the presence of accretion makes photoevaporation an unlikely cause of the inner hole, and giant planet formation thus becomes the most likely scenario once stellar companions have been ruled out.

In 2008, Sewatian et al. announced the discovery of a hot Jupiter orbiting TW Hydra; however, the radial velocity signal was soon shown to be produced by a cool stellar spot (Huelamo et al. 2008). While at the time of this writing no planet has been unambiguously detected within a primordial circumstellar disk, this is an area of intense activity, and it is reasonable to assume that it will not be long before such a discovery is made. Such a discovery would confirm the long suspected connection between transition disks and planet formation and provide an ideal laboratory to study the conditions in which planets are formed with current instruments and telescopes to come.

7.8 Section Summary

- Transition disks can be broadly defined as disks with a significant flux decrement relative to the median SED of CTTSs at any or all infrared wavelengths.
- Transition disks are relatively rare ($\lesssim 10 - 20\%$ of the disk population) as most pre-main sequence stars in nearby-star forming regions have either optically thick disks extending inward to the dust sublimation temperature or no evidence for a disk at all.
- Transition disks present a wide range of SED morphologies and physical properties (e.g., disk masses, accretion rates, and inner hole sizes).
- Transition disk SEDs can result from several physical processes such as grain growth, photoevaporation, dynamical interactions with (sub-)stellar companions, and giant planet formation. All these processes have distinct observational signature and can be distinguished when the right data sets are available.

- There seem to be two *physically* distinct families of transition disks: objects with falling ($\alpha_{\rm excess} \lesssim 0$) and rising ($\alpha_{\rm excess} > 0$) mid-infrared SEDs. The former group has in general been interpreted as evidence for grain growth and dust settling toward the midplane. Objects with rising mid-infrared SEDs, are more consistent with a sharp inner opacity holes due to photoevaporation or dynamical interactions with (sub-)stellar companions or an embedded giant planet.
- Transition disks are excellent laboratories to study disk evolution and planet formation with current and future generations of telescopes.

8 SUMMARY

- SUMMARY FROM OTHER SECTIONS TO BE ADDED
- Circumstellar disks have a median lifetime of $\sim 3\,$Myr with a large dispersion ($< 1 - 10\,$Myr). They dissipate faster around high-mass stars than around solar and lower-mass stars. Medium separation binaries ($r \sim 5 - 100\,$AU) and high radiation environment tend to reduce disk lifetimes.
- Circumstellar disks evolve through a variety of processes, including viscous accretion and spreading, photoevaporation by FUV, EVU, and X-ray radiation from the central star, grain growth and dust settling, and dynamical interaction with (sub)stellar and planetary-mass companions. Viscous accretion and photoevaporation operate in the gas and are the main mechanisms through which primordial circumstellar disks lose mass and eventually dissipate. Dust settling and grain growth operate on the solid particles and are believed to represent the initial steps towards the formation of terrestrial planets and also of giant planets in the core accretion model.
- Most circumstellar disks are likely to go through a slow "mass depletion" phase followed by a rapid "disk dissipation" stage: they first lose mass through viscous accretion and FUV photoevaporation and then dissipate from the inside out through EUV photoevaporation. A wide range in the duration of the "mass depletion" stage and the short time scale of the "disk dissipation" phase weaken any expected correlation between stellar age and disk evolutionary stage. Some disks develop sharp inner holes due to dynamical interactions with (sub-)stellar or planetary-mass companions.
- Transition disks are relatively rare ($\sim 10-20\%$ of disks) and can be broadly defined as disks with a significant flux decrement relative to the median SED of CTTSs at any or all infrared wavelengths. They present a wide range of SED morphologies and physical properties (e.g., disk masses, accretion rates, and inner hole sizes). Their SEDs can result from several physical processes such as grain growth, photoevaporation, dynamical interactions with (sub-)stellar companions, and giant planet formation. They are thus excellent laboratories to study disk evolution and planet formation.

9 FUTURE DIRECTIONS

- *Disk formation* With the high sensitivity and imaging fidelity of *ALMA*, it will be possible to map faint isotopic lines of dense gas tracers and search for small rotationally supported structures in the centers of molecular cores.

Instabilities may be revealed through spiral waves and other asymmetries and can provide an independent dynamical disk mass estimate. Optically thick lines seen in absorption against the disk continuum will show the infall of material from the core. Multi-wavelength continuum imaging will track the increase in the grain size distribution through the process.

- *Peering into the terrestrial planet zone* Very high resolution observations, $\lesssim 0\farcs1$, at wavelengths beyond a millimeter can image optically thin dust emission and resolve structure in the terrestrial planet forming zone, $R \lesssim 10\,\mathrm{AU}$, of disks in nearby star forming regions. The longer the wavelength the observation, the larger the size of the dust grains that can be detected. With the Square Kilometer Array, it will also be possible to measure the distribution of rocks and snowballs up to meter sizes. Together with *ALMA*, resolved images from sub-millimeter to centimeter wavelengths will show the radial variation of grain growth.
- *Disk chemistry* The ability to survey many disks in many lines with *ALMA* will revolutionize the young field of disk chemistry. As different species and transitions are excited in different regions of a disk, such observations will enable a far more complete picture of the gas disk structure to be developed. Observations of $H_2^{18}O$ will reveal the water contect of disks and constrain the location of the snowline in a statistically meaningful sample. The detection of other molecular isotopologues will allow isotopic abundances (and radial gradients) to be measured and directly compared to cosmochemical studies of meteorites.
- *How and when do giant planets form?* While much progress has been made in understanding the structure and evolution of circumstellar disks, this fundamental question still remains unanswered. Detailed studies of embedded (Class I) disks with *ALMA* will help to establish whether massive young disks can be conducive to the formation of giant planets through gravitational instability. Similarly, planet searches in Class II YSOs, and transition disks in particular, with the next generation of large infrared telescopes will identify young giant planets at the last stages of the core accretion process.
- *Toward comprehensive disk evolution models:* To date most disk evolution models have focused on one or two physical processes at a time (e.g., viscous accretion and photoevaporation) while ignoring other equality important ones (e.g., grain growth and dust settling and dynamical interactions with (sub)stellar companions and/or young planets). In reality, however, it is clear that all these processes are likely to operate simultaneously and affect one another, and that any realistic disk evolution model should include all known disk evolution mechanisms.
- *What is the overall evolution of the gas-to-dust mass ratio in cicumstellar disks?* While the evolution of the dust ($r \lesssim 1\,\mathrm{mm}$) content in disks can be traced reasonably well by current (sub)millimeter observations, our current understanding of the evolution of the gas is very limited. Observations of gas tracers with *Herschel* (e.g., [O I] at 63.2 μm), large infrared telescopes (e.g., H_2 at 12.4 and 17.0 μm), and *ALMA* (e.g., rotational lines of CO and its isotopologues) will reveal the evolution of the gas and the gas-to-dust ratio, which is critical to understanding the formation of both terrestrial

and giant planets.

- *Placing our Solar System in context* There are very few well studied disks that appear similar to each other and, whereas there are rough matches to the mass, size, and surface density profile of the MMSN, it is not clear how common these conditions were. As technology improves to allow more refined studies of nearby disks such as TW Hydra and large surveys of more distant star forming regions such as Orion, we will gather the detailed information and large number statistics necessary to understand what is typical and what is atypical about the protosolar nebula.

SIDEBAR ITEMS

- **T Tauri and Herbig Ae/Be stars:** optically visible pre-main sequence stars. T Tauri stars have spectral types M, K, G, F and masses $M_* \lesssim 2\,M_\odot$. Herbig Ae/Be stars are their higher mass counterparts with spectral types A, B and masses, $M_* \gtrsim 2\,M_\odot$.
- **Core accretion model:** giant planets form through a multi-stage process: dust grains grow into rocks and rocks into planetesimals. Gravity helps the larger bodies to accrete solids faster and form the core of a giant planet. Once the core reaches a scale of 10 Earth masses, it starts accreting gas efficiently, and a massive gaseous envelope forms around it.
- **Gravitational instability model:** giant planets form very rapidly ($\sim 10^4$ yr) through the gravitational collapse of perturbations in a young, massive disk.
- **Primoridal disk:** a gas rich disk where the opacity is dominated by dust originated in the interstellar medium (although it may have undergone substantial processing through grain growth and thermal annealing). They are optically thick to *starlight*, and thus reprocess a significant fraction of the stellar radiation ($L_{\rm disk}/L_{\rm star} \gtrsim 10^{-2}$).
- **Debris disk:** a gas poor disk, where the opacity is dominated by second-generation dust produced by the collision of planetesimals. They are optically thin to *starlight*, and hence reprocess a small fraction of the stellar radiation ($L_{\rm disk}/L_{\rm star} \lesssim 10^{-3}$).

Literature Cited

....

Table 1: Classification of Young Stellar Objects

Class	Physical properties	SED slope	Observational characteristics
0	$M_{\rm star} < M_{\rm core}$	–	no optical or near-infrared emission
I	$M_{\rm star} > M_{\rm core}$	$\alpha_{\rm IR} > 0.3$	generally optically obscured
FS		$-0.3 < \alpha_{\rm IR} < 0.3$	intermediate between Class I and II
II	accreting disk	$-1.6 < \alpha_{\rm IR} < -0.3$	strong H recombination lines and UV
III	passive disk	$\alpha_{\rm IR} < -1.6$	no signs of accretion

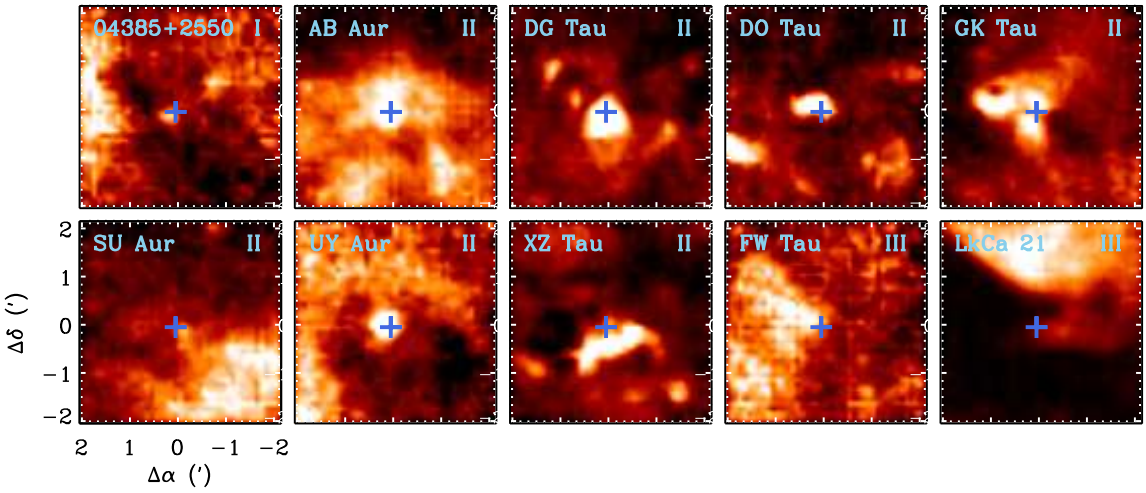

Figure 1: The large scale molecular environment of circumstellar disks in Taurus. Each panel shows a peak temperature map of CO 3–2 from over a $2' \times 2'$ field on a relative scale over 95% of the range from minimum to maximum. The observations were carried out on the JCMT and have a resolution of $15''$. In addition to disk and residual core emission, suggestive morphological connections to the background cloud are seen toward all sources. The names of each source and their infrared evolutionary class, varying from flat spectrum to Class III, are shown at the top of each panel.

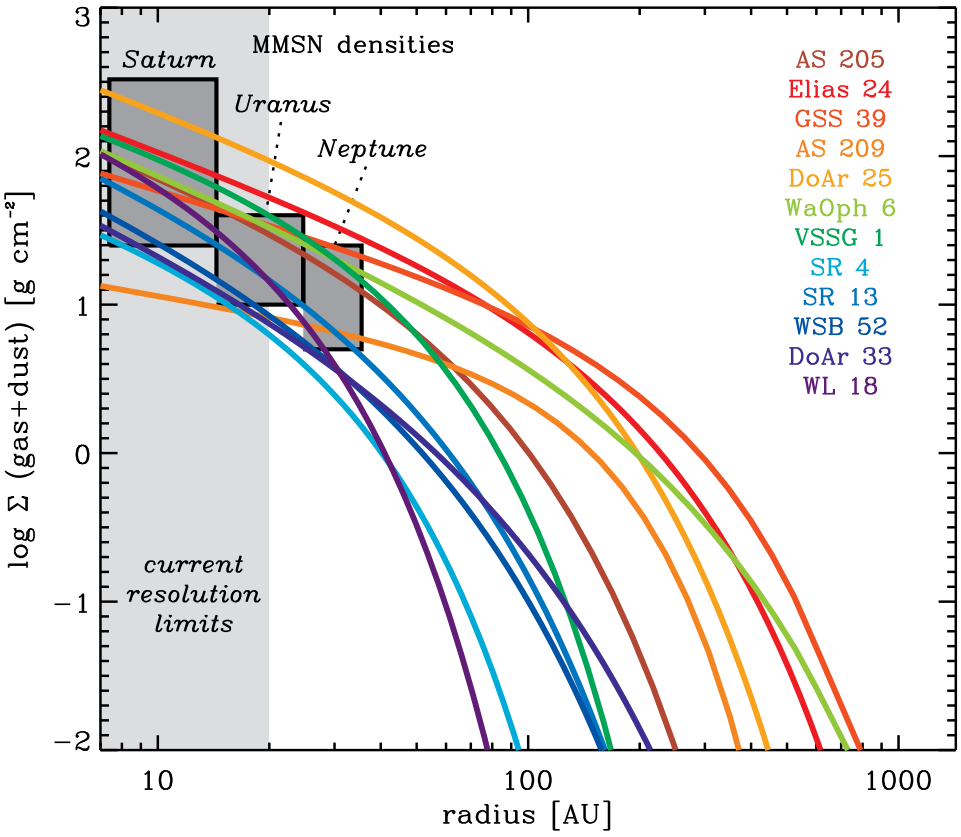

Figure 2: Radial surface density (gas+dust) profiles for Class II disks in Ophiuchus based on fitting an exponentially tapered power law profile to 880 μm visibilities and infrared SEDs. The dark gray rectangular regions mark the MMSN surface densities for Saturn, Uranus, and Neptune.

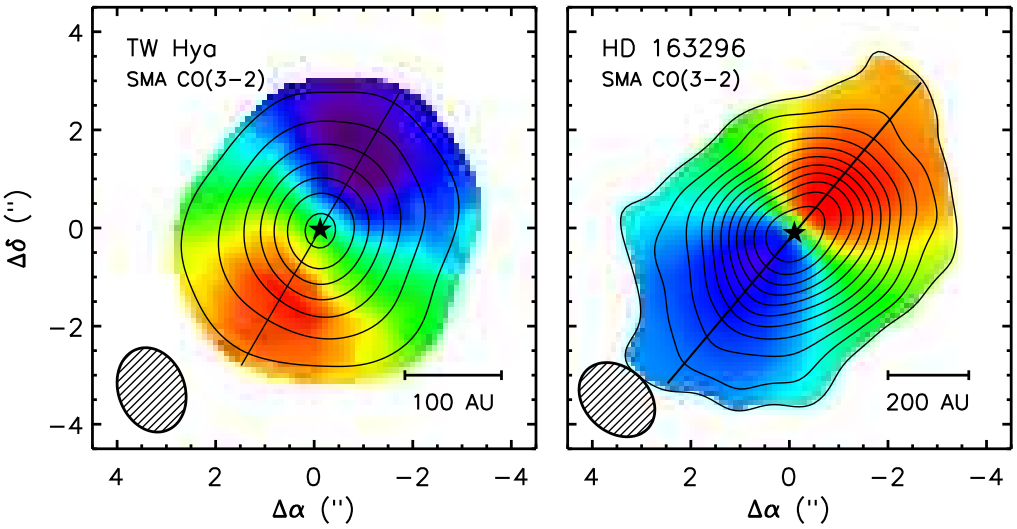

Figure 3: CO(3-2) emission from the disks around TW Hydra (left) and HD 163296 (right) observed with the SMA at a spectral resolution of $44\,\mathrm{m\,s^{-1}}$. The contours show the zeroth moment (velocity-integrated intensity), while the colors show the first moment (intensity-weighted velocity). The synthesized beams are shown in the lower left corner of each panel with a size of $1\farcs7 \times 1\farcs3$ at position angles of 19° and 46° degrees for TW Hydra and HD 163296, respectively. The contours start at 3σ and increase by intervals of 2σ, where the rms noise $\sigma = 0.6\,\mathrm{Jy\,beam^{-1}}$.

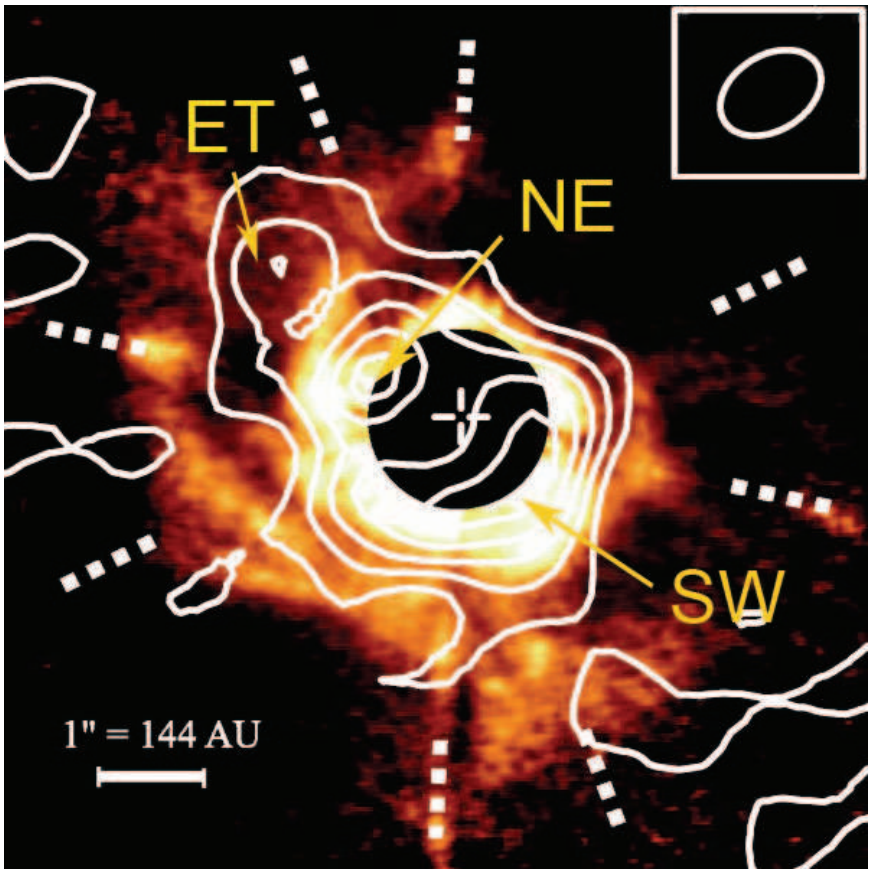

Figure 4: Asymmetries in the AB Aur disk. The white contours show 880 μm emission and are overlaid on a near-infrared coronagraphic scattered light image. The occulted center of the near-infrared image has been blacked out but the sub-millimeter image clearly shows an inner hole. Both images show strong asymmetries that indicate strong dynamical perturbations (from Lin et al. 2006).

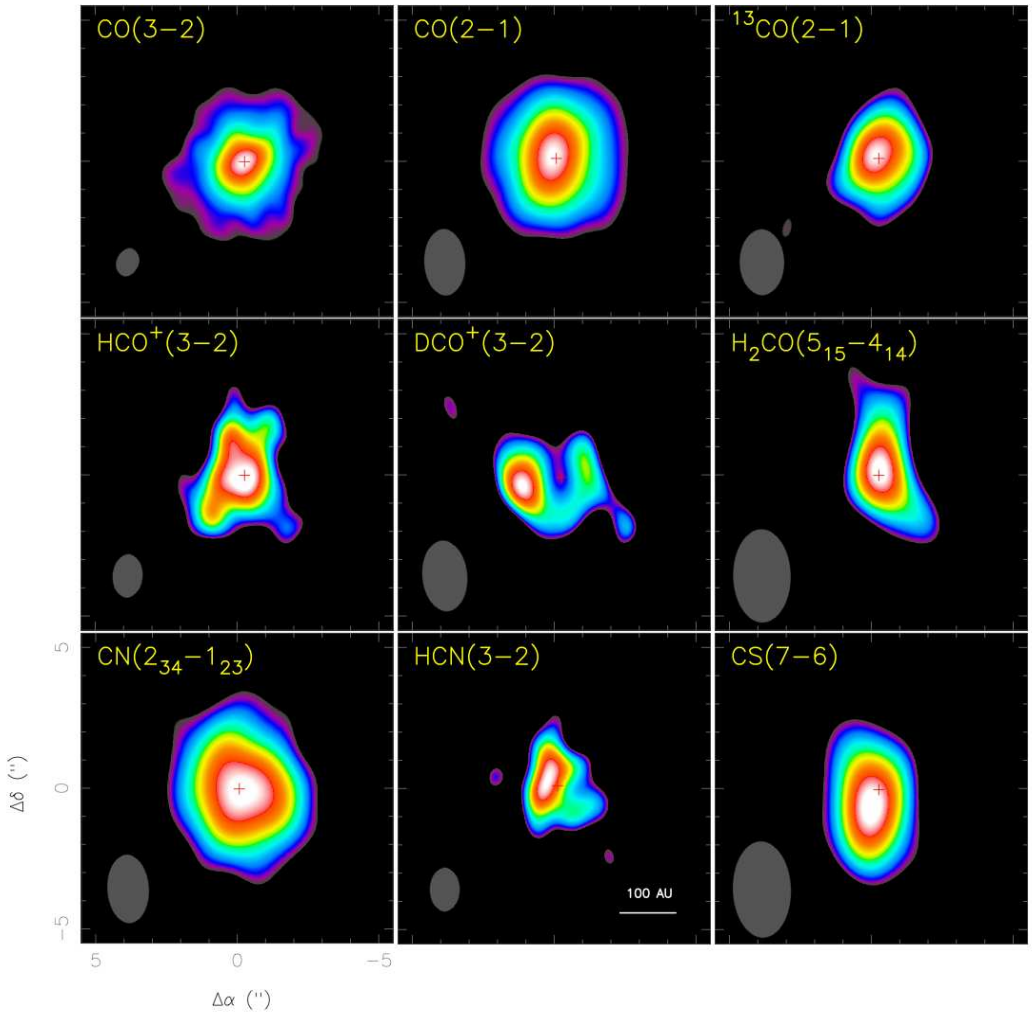

Figure 5: Sub-millimeter spectroscopy of molecular rotational lines in the chemically rich nearby TW Hydra disk. These observations, made with the *SMA* are at a range of resolutions, shown in the lower left corner of each panel. The nearly face-on disk generally shows centrally peaked emission except for the DCO^+ line which peaks in a ring where the CO freezes-out.

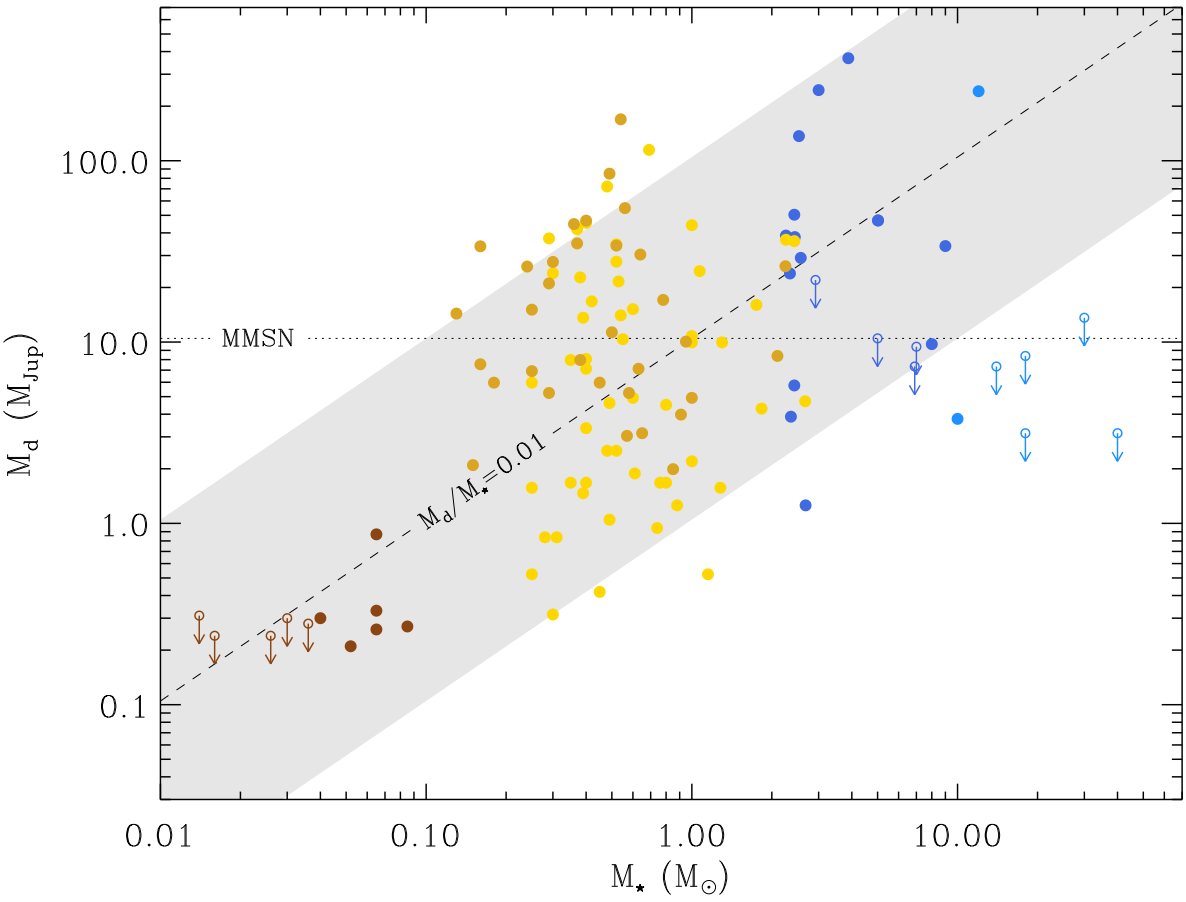

Figure 6: The variation of protoplanetary disk mass with the mass of the central star. The dashed diagonal lines delineates where the mass ratio is 1%, and is close to the median of the detections. Almost all the disks around stars with masses $M_* = 0.01-10\,M_\odot$ lie within the grey shaded area, ± 1 dex about the median. The exception are O stars where no disks are detected at (sub-)millimeter wavelengths, indicating either very short disk lifetimes or a different star formation scenario.

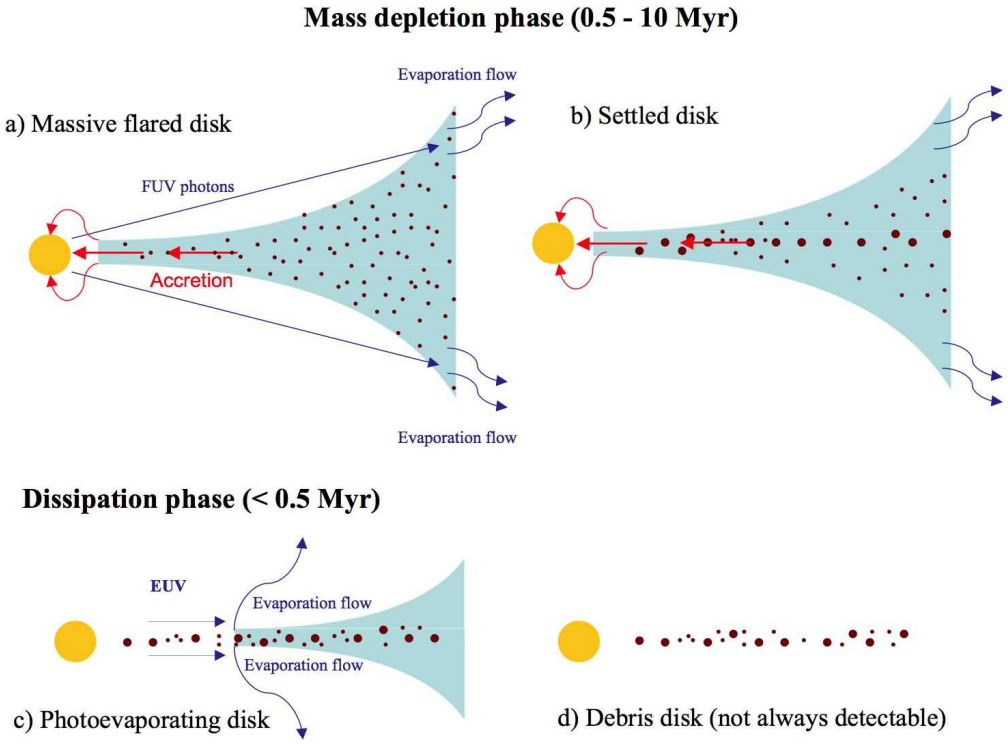

Figure 7: The evolution of a typical disk. (a) Early in its evolution, the disk loses mass through accretion onto the star and FUV photoevaporation of the outer disk. (b) At the same time, grains grow into larger bodies that settle to the mid-plane of the disk. (c) As the disk mass and accretion rate decrease, EUV-induced photoevaporation becomes important, the outer disk is no longer able to resupply the inner disk with material, and the inner disk drains on a viscous timescale ($\sim 10^5$ yr). An inner hole is formed and the disk quickly dissipates from the inside out. (d) Once the remaining gas photoevaporates, the small grains are removed by radiation pressure and Poynting-Robertson drag. Only large grains, planetesimals, and/or planets are left (i.e., a debris disk).

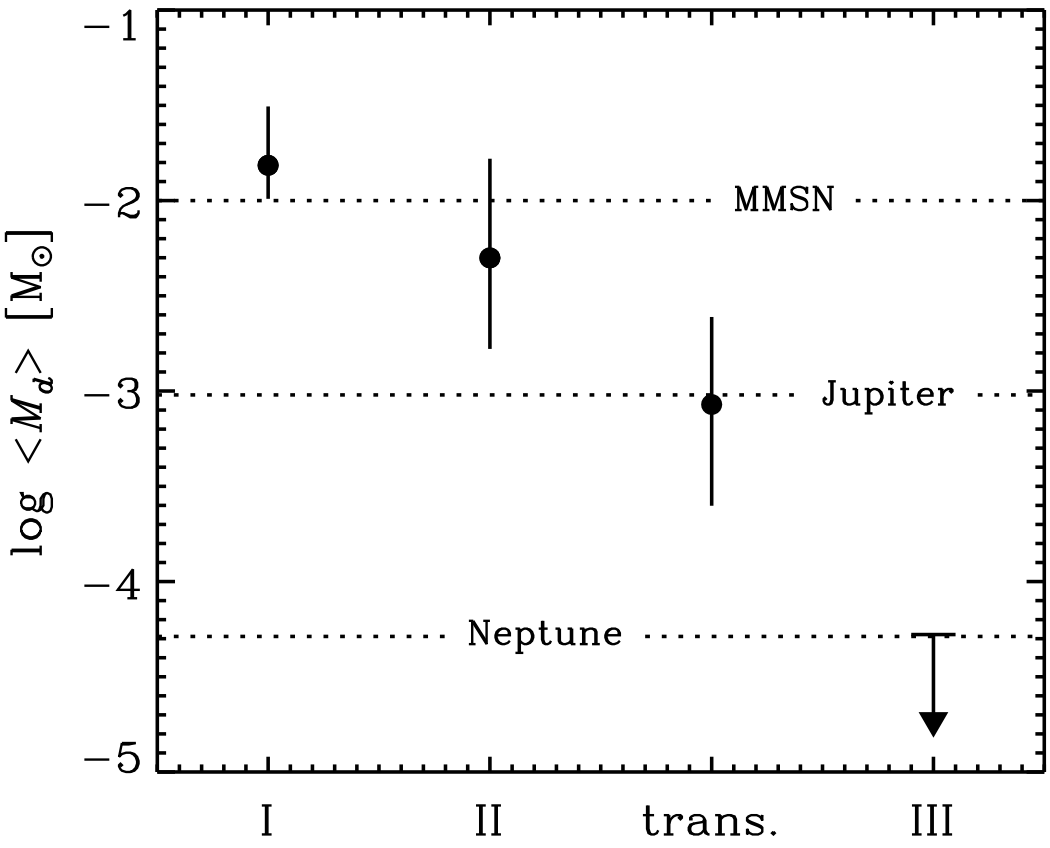

Figure 8: PLACEHOLDER: Evolution of the median disk masses across the empirical sequence defined by the shape of the infrared SED.

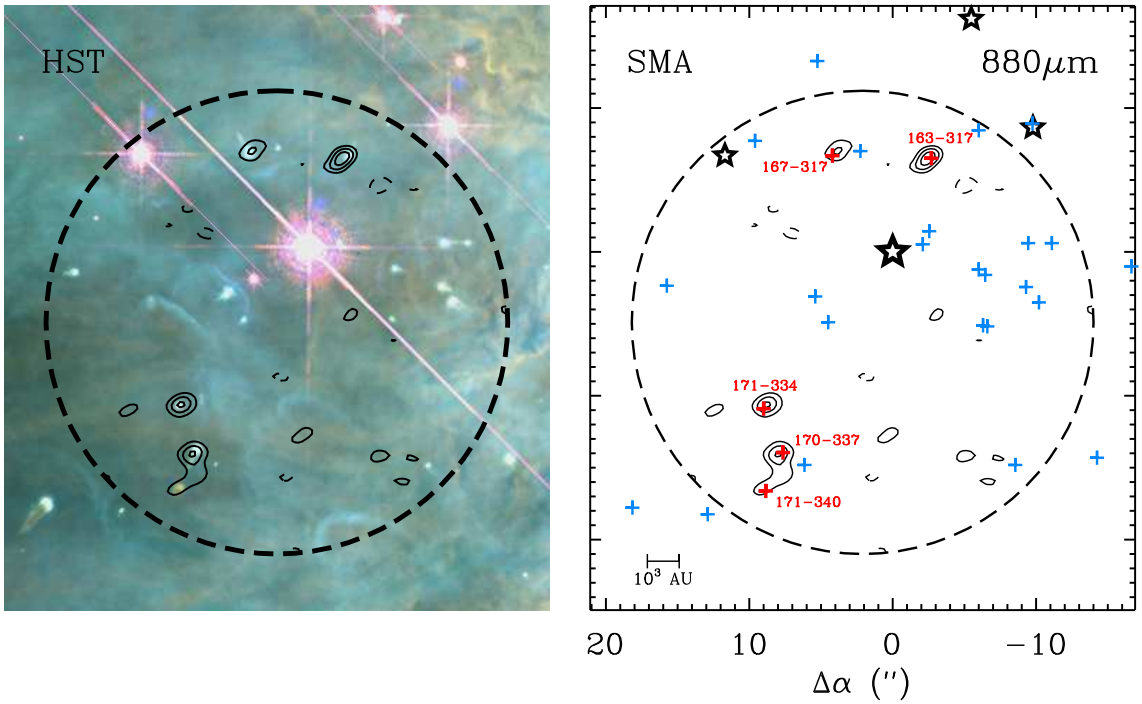

Figure 9: PLACEHOLDER: Optical and submillimeter image of Orion proplyds

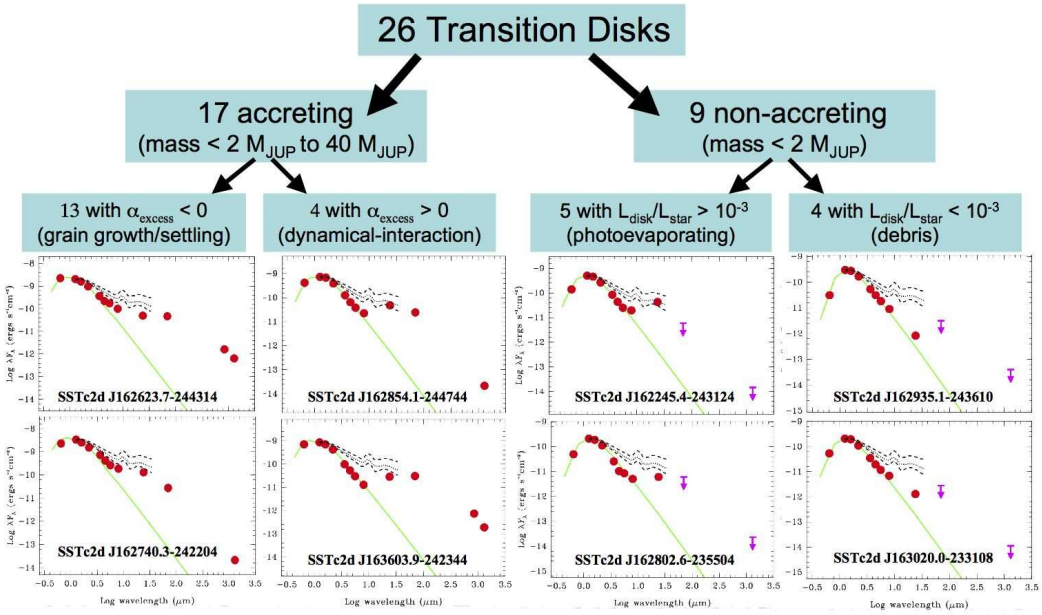

Figure 10: The diversity of transition disks SEDs. (a) The SED of A typical weak-excess, anemic, or homologously depleted disk. It shows a significant flux decrement with respect to the typical SED of an accreting T Tauri star (hashed region). (b) The a SED of a cold disk that can also be classified as a "classical" transition disks based on the lack of near-IR excess. (c) The SED of a cold disk with little near-IR emission and a strong 10 μm silicate feature. (d) The SED of a cold disk that can also be considered a pre-transition disk because its SED can be modeled with an optically thin gap separating optically thick inner and outer disk components. Figure adapted from Najita et al. (2007).

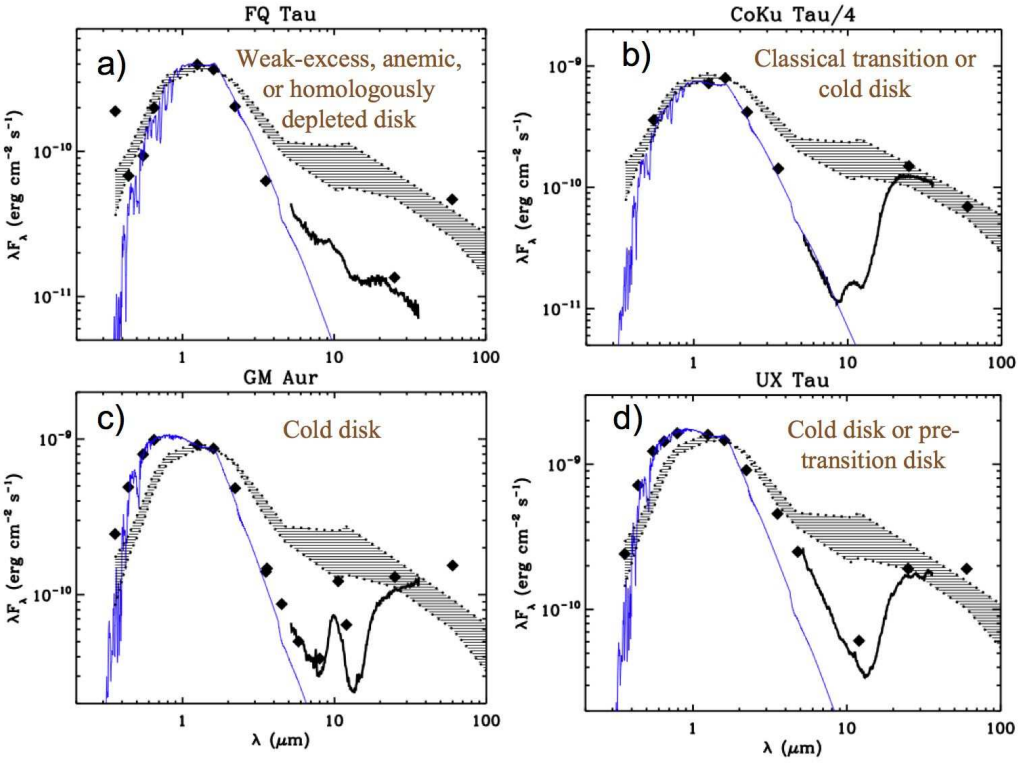

Figure 11: The properties of the Ophiuchus transition disks studied by Cieza et al. (2010). Accreting objects with falling SEDs between 8 and 24 μm ($\alpha_{\rm excess} \lesssim 0$) are consistent with grain growth and dust settling. Accretion objects with raising SEDs between 8 and 24 μm ($\alpha_{\rm excess} > 0$) are more consistent with sharp, dynamically induced inner holes. The low-mass ($< 2\,M_{\rm Jup}$), non-accreting disks in their sample are most likely to be photoevaporating primordial disks or gas-poor debris disks (see lower panel in Figure 10). Their fractional disk luminosities ($L_{\rm disk}/L_{\rm star}$) can be used as a preliminary diagnostic to distinguish between the two scenarios. On the one hand, debris disks are optically thin to stellar radiation and thus intercept and reemit a small fraction of the starlight. On the other hand, primordial photoevaporating disks should have fractional disk luminosity values intermediate between those of debris disks and optically accretion disks. The dotted lines correspond to the median SED of K5-M2 CTTSs calculated by Furlan et al. (2006). The dashed lines are the quartiles.

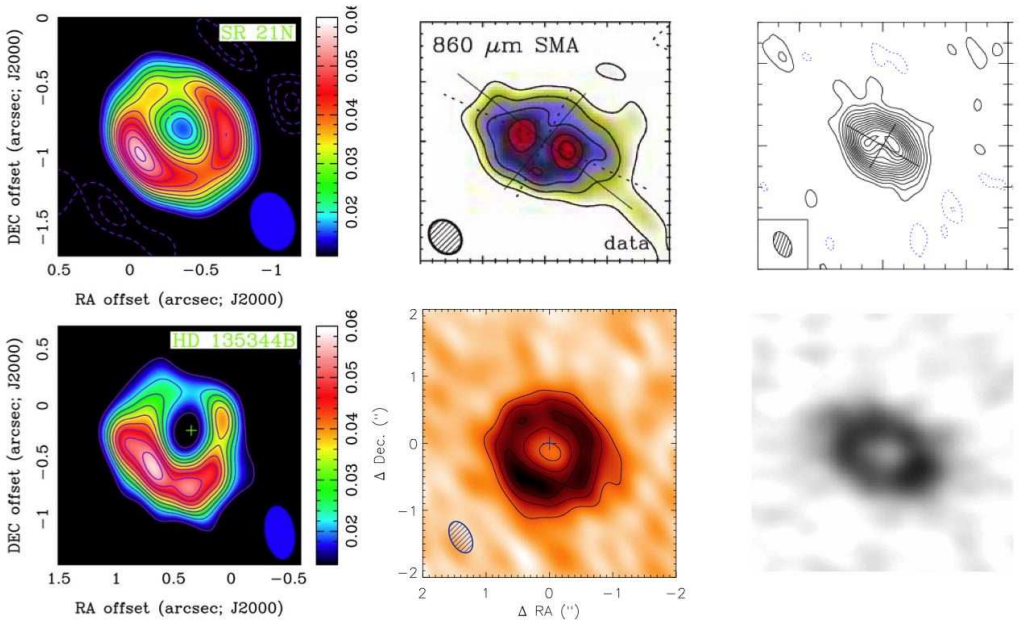

Figure 12: PLACEHOLDER: Montage of resolved images of transition disks.